Simulation of flow redistribution in 7 x 7 ballooned fuel bundle experiments using DRACCAR code

J.E. Luna Valencia, A.V.S. Oliveira, Tony Glantz, Alexandre Labergue, S. Leclerc, Michel Gradeck

Simulation of flow redistribution in 7x7 ballooned fuel bundle experiments using DRACCAR code

J.E. Luna Valencia[a,b], A.V.S. Oliveira[b], T. Glantz[a], S. Leclerc[b], A. Labergue[b], M. Gradeck[b,*]

[a] *IRSN, PSN, B.P. 3, 13115 Saint Paul-Lez-Durance, France*
[b] *Université de Lorraine, CNRS, LEMTA, F-54000 Nancy, France*

Abstract

IRSN has developed the DRACCAR code in order to model loss of coolant accidents (LOCA) in a light water nuclear reactor. The physics during a hypothetical loss of coolant accident involves several phenomena such as heat and mass transfers, fluid dynamics, mechanics and chemistry. Even if the modeling requires these conjugated processes, it is important to validate them separately first. Clad ballooning can occur during a LOCA, leading to flow redistribution between sub-channels. In this paper, we present DRACCAR simulations of the fluid dynamics in two 7 x 7 ballooned bundles with different blockage ratios and ballooned lengths and with two different flow rates, one laminar and the other turbulent. DRACCAR results for the axial velocities in specific sub-channels are compared to experimental data obtained by MRI techniques on the MASCARA facility. The present results show that DRACCAR is capable of predicting correctly the velocity profiles for both bundles and flow rates. The axial velocity is, in general, well estimated by DRACCAR, especially for the intact and less-blocked sub-channels. DRACCAR also performed well for the most blocked sub-channel for both bundles, performing better for the most blocked one, which ensures DRACCAR fluid dynamics calculations in the most critical regions in LOCA conditions.

Keywords:
LOCA, Nuclear reactor, Clad ballooning, Thermal-hydraulics, Reflooding, Magnetic Resonance Imaging

1. Introduction

One hypothetical accident that is considered for the design of the safety systems of pressurized-water reactors (PWR) is the Loss of Coolant Accident, commonly referred to as LOCA. During the course of such an accident, the fuel rods heat dissipation can be highly degraded and the fuel assemblies' temperature rapidly increases. In some cases, it leads to the ballooning or burst of some of the pressurized fuel rods and the formation of blocked sub-channels (Fig. 1) [1]. The emergency core cooling system (ECCS) is designed to inject fresh water into the nuclear reactor's core to impede the fuel assemblies to reach prohibitive temperatures. This step is known as the reflooding phase. Because of the high temperature of the fuel rods, the injected water partially evaporates and a steam-droplet two-phase flow is created downstream of the water level. This phenomenon plays a very important role in the coolability of the regions not yet immersed in water.

Different thermal-hydraulic studies have been carried out to characterize this two-phase flow and its cooling capacity: the droplets' size across spacer grids under reflood conditions [2, 3], the modeling of droplets breakup and

*Corresponding author
Email address: michel.gradeck@univ-lorraine.fr (M. Gradeck)

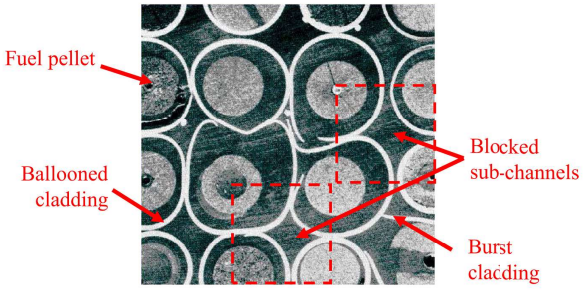

Figure 1: Picture after PHEBUS in-pile LOCA experiment showing the clad ballooning and the formation of blocked sub-channels ([1]).

entrainment during the reflooding phase [4, 5] and the droplets dynamics and heat transfer between the flow and the nuclear rods at sub-channel scale [6, 7]. Furthermore, the steam flow rate entering the blocked sub-channels is decreased due to its preferential deviation to less deformed sub-channels [8]. Ruyer et al. [9] observed in a CFD analysis that with this steam deviation, the large droplets tend to continue their path toward the blocked sub-channel because of their high inertia. Nevertheless, this is still particularly critical because wall-to-steam convection is highly decreased, as this is the most important heat dissipation process during a LOCA [10, 11]. For this reason, the thermal-hydraulics in blocked sub-channels raises concerns on the core coolability to guarantee nuclear safety [12].

In order to increase the knowledge on the cooling of a reactor's core during a LOCA, the French Institut de Radioprotection et de Sûreté Nucléaire (IRSN) launched the PERFROI project intending to perform high-quality experiments for better understanding the thermal-hydraulics and thermomechanics during a LOCA. In the thermal-hydraulics axis, the main experiment (named COAL[1] [13, 14]) consists of a bundle of electrically heated rods, with the blockage region simulating clad ballooning and fuel relocation (balloons filling up with fuel pellets, associated with a possible power profile modification [15–17]), using a 7 x 7 bundle geometry at full-length scale. The test section instrumentation counts with many thermocouples placed on the sheaths, on the housing and in the flow. Although COAL experiments allow the thermal-hydraulics characterization during the reflooding phase, information on the heat transfer and fluid dynamics processes is hidden in this large-scale experiment. For this reason, additional experimental campaigns were carried out to complement COAL with information on the two-phase flow heat transfer and hydraulics. On the one hand, experiments with COLIBRI[2] experimental apparatus [6, 7] resulted in a precise characterization of the heat transfer phenomena by analyzing a steam-droplets flow within a vertical tube in LOCA conditions at the sub-channel scale. On the other hand, using MRI techniques, the experimental campaign MASCARA[3] [18, 19] provided valuable information on the flow redistribution in the presence of ballooned zone within several 7 x 7 bundles. The geometries tested in MASCARA were very similar to the test sections to be used in COAL experiments. Therefore, while COLIBRI contributed to the analysis of the thermal phenomena and the droplets dynamics, MASCARA campaign isolated the hydraulics from thermal effects and analyzed the flow behavior when passing through spacer grids and ballooned fuel rods.

All the effort spent in experimental campaigns is justified because they serve to acquire knowledge of the involved

[1]COAL: **CO**olability of a fuel **A**ssembly during **L**OCA
[2]COLIBRI: **CO**o**LI**ng of **B**lockage **R**egion **I**nside a PWR Reactor
[3]MASCARA: **M**RI of **A**ssembly **S**ub-**C**hannels for the **A**nalysis of **R**eactor **A**ccidents.

physical phenomena and integrate it into computer codes such as DRACCAR[4], an IRSN's code that describes the 3D thermomechanical behavior and reflooding of a fuel assembly including its coolability as well as its embrittlement during a LOCA. The code evaluates the blockage ratio associated with deformed fuel rods and their impact on core cooling. Also, DRACCAR simulates the uncovery (dewatering) phase of cooling accidents affecting spent fuel pools. This calculation implies complex computations involving multi-phase flow, coupled with heat transfers, chemical reactions, mechanical strain, and fuel relocation. In thermal-hydraulics simulations, DRACCAR is coupled to two different codes, CESAR [20] and CATHARE-3 [21].

DRACCAR simulations of COLIBRI experiments have already been performed [10] and very good agreement has been observed, even though the heat transfer by impact of the droplets has been neglected. The next step, before the simulation of COAL experiments with DRACCAR, is the simulation of the MASCARA hydraulics experiments, object of the present paper. Although Oliveira et al. tested several geometries and flow rates [18, 19], we compare herein calculations and experimental results for two flow rates and two bundles: one bundle with 90% of blockage ratio and 240 mm of blockage length and one with 61% of blockage ratio and 100 mm of blockage length, both with flow rates of 50 and 245 lpm. In this study, the DRACCAR/CATHARE-3 coupling is used in the different simulations.

2. MASCARA: experimental apparatus and procedure

MASCARA device has been developed to measure three-component velocity fields in fuel rods bundles having ballooned zones using magnetic resonance velocimetry (MRV). More than 1,000 velocity fields were obtained with seven different bundles and four different flow rates, some results presented in detail in previous studies, like comparing the flow in an intact bundle and a ballooned one [19] and analyzing parametric effects on the flow redistribution because of clad ballooning [18]. Detailed information regarding the measurement techniques, the MRV sequence and parameters, data reduction and uncertainties are available in these previous works. In this paper, we present only the main aspects concerning the test section that are important when comparing the experimental results with DRACCAR simulations.

MASCARA's experimental bench is schematically represented in Fig. 2, consisting of a regular single-phase hydraulic circuit with a screw pump connected to a damper in order to assure a stable flow in all the circuit, pressures transducers for safety purposes, an electromagnetic flowmeter to measure the water flow rate, which is later used for validating the MRV measurements, and the test section. This one consists of a 7 x 7 representative test bundle, which is inserted into a radiofrequency (RF) coil and this assembly is, in turn, inserted into the MRI scanner. The intact rods were made of polycarbonate tubes, while the ballooned rods were constructed by 3D printing (FDM - fused deposition modeling) using PLA as the base polymer. Furthermore, the four spacer grids were made of Inconel and they had the same material and geometry used in COAL experiments [1]. These grids were not made of a ferromagnetic material; however, they still disturbed the magnetic field and impeded accurate velocity field measurements by 4 cm close to them.

All the bundles tested by Oliveira et al. [18] had 49 elements arranged in a 7 × 7 structure, having thirty tubes

[4]DRACCAR: **D**éformation et **R**enoyage d'un **A**ssemblage de **C**rayons **C**ombustibles pendant un **A**ccident de **R**efroidissement

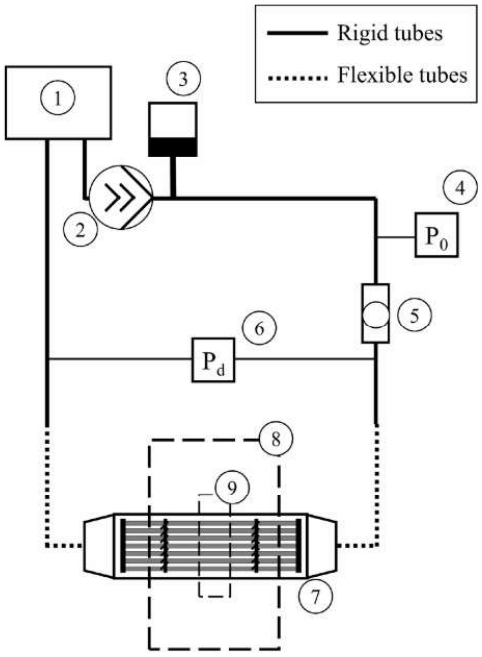

Figure 2: Hydraulic circuit of MASCARA: 1) water tank, 2) eccentric screw pump, 3) damper, 4) absolute pressure transducer, 5) electromagnetic flowmeter, 6) differential pressure transducer, 7) test section, 8) MRI scanner, 9) radio- frequency (RF) coil. ([19]).

with 9.5 mm diameter to represent intact fuel rods, sixteen ballooned tubes, and three tubes with a 12.45 mm diameter to represent guide tubes. In this study, we chose two bundles having two different blockage ratios and two different blockage lengths, named G61%/100mm and G90%/240mm, to compare with DRACCAR simulations. The blockage ratio τ_b describes the reduction in the cross-sectional area because of the cladding ballooning and is defined by:

$$\tau_b = 1 - \frac{S_b}{S_0} \tag{1}$$

where S_b and S_0 are the flow passage areas of a blocked and an intact sub-channel, respectively. The first bundle, G61%/100mm, represents the case where the blocked sub-channels are formed by four ballooned rods that touch their neighboring rods without losing the circular shape ($\tau_b = 61\%$ in Fig. 4), with a blockage length of 100 mm. The second bundle, G90%/240mm, represents a severe blockage ratio and length, as mentioned by Grandjean [22]. In this case, the blocked sub-channels are formed by ballooned fuel rods with a squared shape and rounded corners, due to joint deformation with neighboring rods ($\tau_b = 90\%$ in Fig. 4). Therefore, in the ballooned zone (for τ_b equal to both 61% and 90%), the flow within blocked sub-channels is isolated from neighborhood sub-channels with both bundles.

Figure 3 shows the side view of these two test section configurations and the position of the spacer grids and the ballooned zone, with their values given in Table 1. The first and the last spacer grids do not have mixing vanes, while the two in the middle have them with remarkable performance to homogenize the flow, as described in previous studies [19]. The distance of 522 mm between the two mixing spacer grids in the middle (E – A) was fixed because it is approximately the same distance found in typical French PWR's. Figure 4, in turn, shows the bundles

cross-sectional views in the intact and ballooned zones, the first only having intact sub-channels (no ballooning) and the second having the balloon whose shape corresponds to the bundles blockage ratios (61% and 90%).

Table 1: Dimensions of the tested bundles as shown in Fig. 3 (in mm).

Bundle	τ_b	L_b	A	B	C	D	E	F	E-A
G61%/100mm	61%	100	252	444[a]	479	614[a]	774	1073	522
G90%/240mm	90%	240	282	370	435	740	803	1072	521

[a] In our previous study [18], these dimensions were incorrectly presented (difference of 10 mm). These are the correct values.

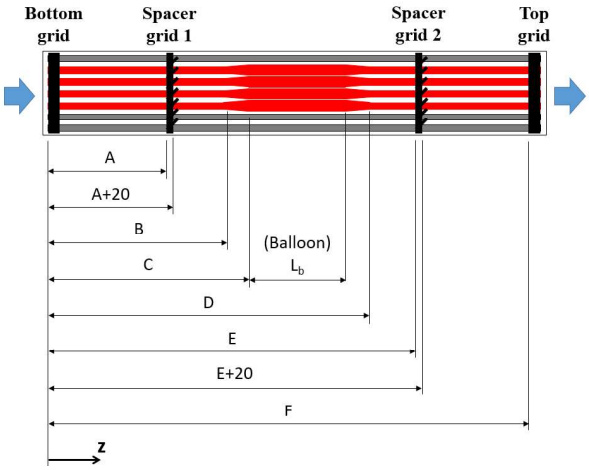

Figure 3: Axial positions of the grids and the balloon in the bundles.

Between the intact and the ballooned regions, there is a transition zone (Fig. 5). For the G61%/100mm bundle with a blockage ratio of 61%, the fuel rods cross-section increases keeping the circular shape and the transition finishes where they are in contact. The length of this transition is 35 mm. For the case of the G90%/240mm bundle with a 90% blockage ratio, there is a first transition like the one in the G61%/100mm bundle and a second transition zone, which is 30 mm long, where the fuel rods shape continues deforming progressively until reaching the final cross-section shown in Fig. 4. For both bundles, there is another transition zone downstream of the balloon, exactly like the first but mirrored.

As mentioned at the beginning of this section, MRV was the technique we used to measure the velocity fields in these bundles. We used a typical gradient-echo pulse sequence with an additional flow encoding sequence. The pixel resolution was 0.47 x 0.47 mm^2 and the experimental procedure ensured the velocity uncertainty in one pixel to be about 20% of the bulk mean velocity [19]. However, to compare the experimental results with DRACCAR simulations, we must take the mean axial velocity within a sub-channel. In this case, the uncertainty of this mean velocity is reduced to 10% of the flow mean velocity, as discussed by Oliveira et al. [18].

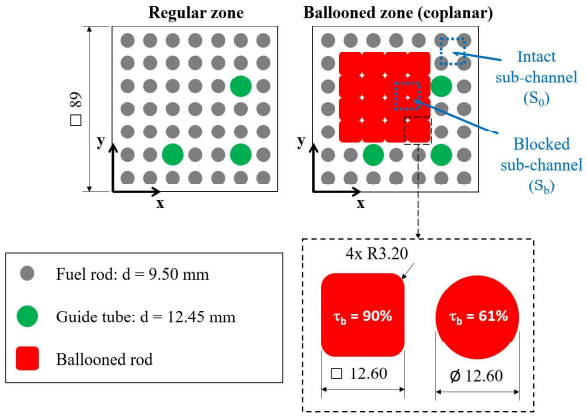

Figure 4: Section view in the intact and ballooned zones, with evidence on the ballooned fuel rods' shapes for 61% and 90% blockage ratios ([19]).

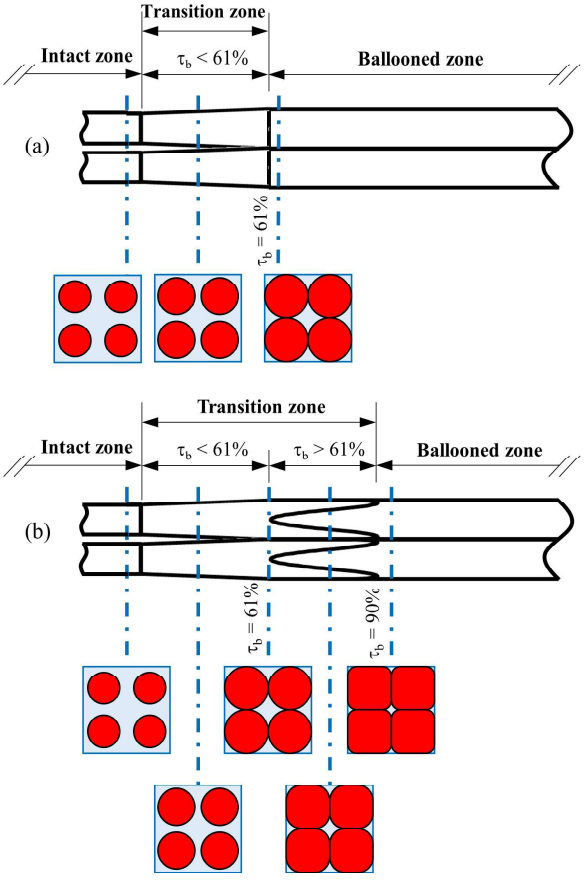

Figure 5: Transition from regular to ballooned zone for both bundles: a) G61%/100 mm; b) G90%/240mm.

3. DRACCAR: details of the simulation

3.1. Modeling concept

DRACCAR is a code from the FUEL+ software platform developed by IRSN since 2008 to simulate the 3D thermo-mechanical deformation and the reflooding of fuel rods during a LOCA (among other phenomena). DRACCAR allows

modeling problems with different scales, from a single fuel rod or fuel assembly to the entire reactor's core or spent fuel pool. Moreover, this code can perform calculations including fuel assembly components like control rods, fuel rods (modeling both the stack of fuel pellets and the cladding), instrumentation tubes, guide tubes, and spacer grids. To achieve this, DRACCAR couples two codes: a thermo-mechanical code ICARE3D and one of the two different thermal-hydraulic codes, CESAR and CATHARE-3 [16]. In the present study, we coupled DRACCAR with CATHARE-3 and disabled the thermo-mechanical package as it was unnecessary to simulate MASCARA experiments.

For the thermal-hydraulics calculations, DRACCAR relies on a 3D structured mesh with hexahedral elements. In the transverse direction, each element contains one sub-channel, which means that DRACCAR does not calculate velocity profiles within the sub-channel. On the other hand, the sub-channels are meshed in the axial direction. Hence, the mass and momentum balance equations are solved for each element. Although the simulation in this study in single-phase, DRACCAR can also perform two-phase flow calculations.

3.2. Simulation domain and conditions

The main objective of simulating MASCARA experiments using DRACCAR is to validate the fluid dynamics models implemented in the code by comparing the calculated and measured fluid velocities upstream, within, and downstream of the ballooned zone. Thus, the simulation domain is restricted to the bundle part downstream of the first mixing spacer grid until the top grid of the test section (Fig. 6). The inlet boundary condition was set for each sub-channel as the velocity measured experimentally in MASCARA and the outlet pressure value was set to the atmospheric pressure (relative pressure equal to zero).

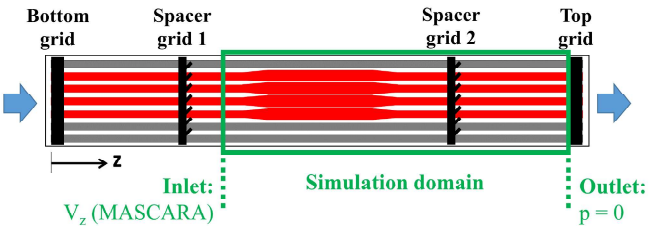

Figure 6: Simulation domain of the present study.

The exact geometries of the intact fuel rods, guide tubes and housing used in MASCARA experiments were simulated with DRACCAR, which means the fluid passage section areas (in all the three directions) were as well correctly represented. The axial ballooned rods shape could not be simulated continuously over the axial DRACCAR meshing. Thus, their complex geometry was modeled in order to preserve the exact fluid passage area at all the mesh faces, as shown in Fig. 7. This modeling was performed following several steps. First, we calculated the volume of each ballooned rod forming a given sub-channel. Then, this rod volume was divided by the element dimension in a given direction to obtain the wall section area. Finally, this section area was subtracted to the total element section area to obtain the precise fluid section area for the concerned face. With this choice, in the axial direction, the diameter of the tube was precisely equal to 12.6 mm between the two transitions (Fig. 7).

For the radial singular pressure drop, a coefficient k is imposed at each vertical mesh face and is determined

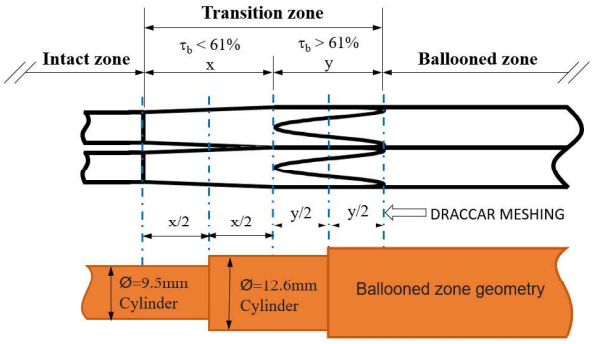

Figure 7: Example of balloon modeling with DRACCAR.

automatically by DRACCAR using a modified Idel'cick equation [23]:

$$k = 0.228 \left(\frac{p}{d} - 1 \right)^{-0.5} \tag{2}$$

where p and d are the pitch and the external rod diameter respectively. Finally, some number of the domain discretization are: for the G61%100mm bundle, we used 24 axial elements, of which 8 correspond to the transition and ballooned zones; and for the bungle G90%/240mm we used 41 axial elements, 14 of them being in the transition and ballooned zones.

3.3. DRACCAR/MASCARA comparison

Oliveira et al. [19] presented velocity fields like the example in Fig. 8a (without transverse velocities), the colored bar referring to the magnitude of the axial velocity V_z (z-direction, Fig. 6) normalized with the bulk mean velocity $\widetilde{V}_{ref}$. Nevertheless, DRACCAR simulations only provide mean velocities for each sub-channel, i.e. without detailing the velocity field within the sub-channels. For this reason, MASCARA results of velocity fields were re-processed to obtain the mean axial velocity for each sub-channel. Fig. 8b presents the same velocity field shown in Fig. 8a but now with the normalized mean axial velocity for each sub-channel, which can be compared with DRACCAR simulations. In addition, we used two flow rates for the DRACCAR validation: 50 lpm and 240 lpm, corresponding to a Reynolds number of 1936 and 9599 respectively (laminar and turbulent flow).

Comparing visually the velocity fields as in Fig. 8 or presenting velocity profiles for all the 64 sub-channels would not be practical nor simple to validate the DRACCAR simulations. Therefore, we chose specific sub-channels to compare MASCARA and DRACCAR results (Fig. 9), each one with specific blockage and location characteristics as listed below:

- **A**: a sub-channel with the highest blockage ratio, in the center of the ballooned zone;
- **B**: a moderately blocked sub-channel between two intact rods and two ballooned rods;
- **C**: a moderately blocked sub-channel between one guide tube, one intact rod, and two ballooned rod;
- **D**: an intact sub-channel.

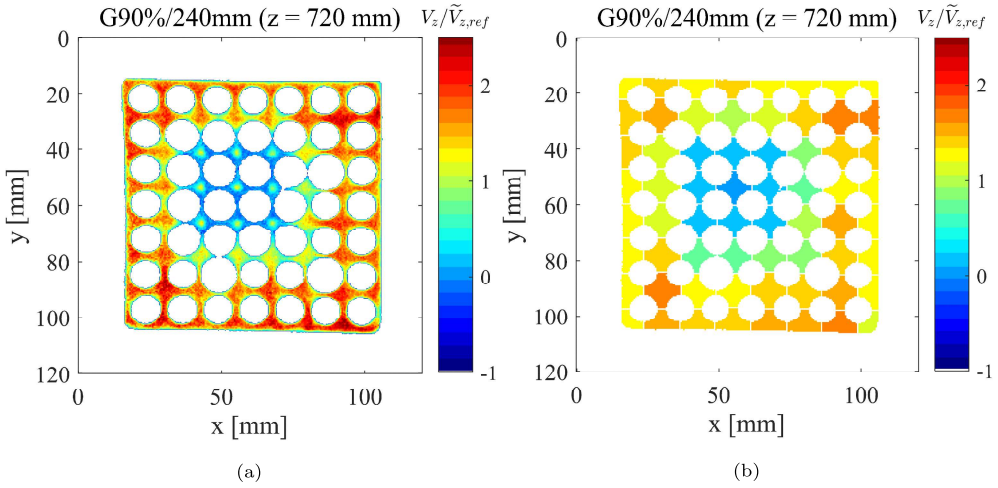

Figure 8: Example for G90%/240mm bundle at 50 lpm of: (a) a normalized axial velocity field obtained by MRI techniques (MASCARA result), and (b) its corresponding normalized mean axial field for each sub-channel for comparison with DRACCAR simulation.

These sub-channels present axial velocity profiles with different behaviors that worth the discussion in this paper. Other sub-channels could also be used in the results presentation, like those partially blocked in the corners of the ballooned zone (for example, the one between D and D' or the one at two sub-channels above C) or those neighboring the housing. They were not used because the first is less critical than the chosen partially blocked sub-channels and the latter presented practically the same velocity profile of an intact sub-channel.

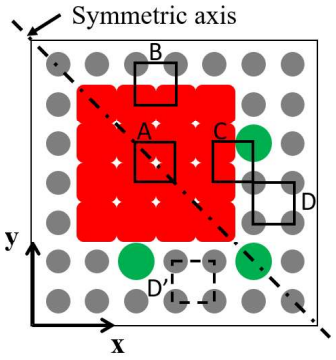

Figure 9: Sub-channels chosen for this study and the bundle symmetry axis, showing an example of symmetric sub-channels (D and D').

The tested geometry was designed to be symmetric to an inclined axis (Fig. 9), which should result in a velocity field as well symmetric to the same axis. However, the bundles used in MASCARA could be slightly misaligned inside the housing [19] and this would favor the axial flow in one sub-channel compared to its symmetric one, although the difference is negligible most of the times. We present examples of this result with the G90%/240mm bundle at the beginning of the results presentation. To reduce experimental biases because of the bundle misalignment and to better validate DRACCAR simulations, we used the mean velocity of the two symmetric sub-channels of MASCARA results. Moreover, averaging the sub-channel velocities reduces the experimental uncertainty because considering more pixels in the averaging population reduces the measurement noise. Figure 9 presents an example of symmetric sub-channels (D and D'), so the experimental results presented in the next section for this sub-channel are actually

the average of these two sub-channels.

4. Results and discussion

We present herein the results as axial velocity profiles for the chosen sub-channels shown in Fig. 9 and for both bundles (G61%/100mm and G90%/240mm) and flow rates (50 and 245 lpm). For a better comparison of MASCARA and DRACCAR results, we normalized both axial positions according to the zone in the bundle and the sub-channels' axial velocities. The first normalization was done by taking the position within a given zone (intact, transition or balloon) and dividing it by the length of this zone. Meanwhile, the axial velocity normalization was performed according to the following equation:

$$V_{z,n} = \frac{V_z - V_{min}}{V_{max} - V_{min}} \tag{3}$$

where V_{min} and V_{max} are, respectively, the minimum and maximum axial velocities either simulated in DRACCAR or obtained in MASCARA, resulting in $V_{z,n}$ always between 0 and 1.

As mentioned in the previous section, we present in Fig. 10 results for symmetric sub-channels with the G90%/240mm bundle for the two tested flow rates. Because DRACCCAR simulations result in perfectly matched axial velocity profiles for symmetric sub-channels, only one of its curves is presented in the figure. For MASCARA results, the axial velocities of symmetric sub-channels are very similar for both flow rates but do not match perfectly, which is natural in experiments. Hence, using average values for MASCARA axial velocities to compare with DRACCAR simulations is reasonable to reduce experimental imperfections, even if they are very small.

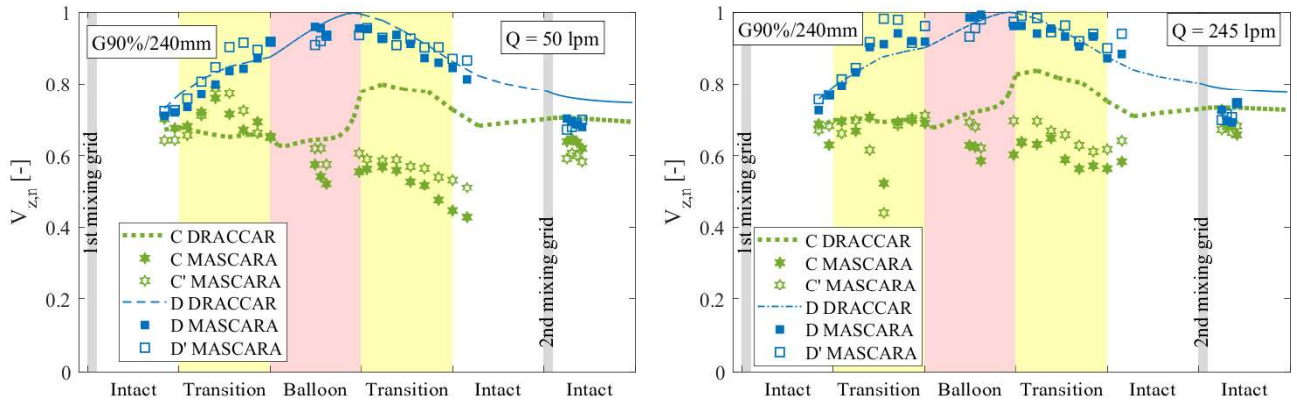

(a) (b)

Figure 10: Comparison of axial profiles in symmetric sub-channels for the G90%/240mm bundle: (a) 50 lpm, and (b) 245 lpm.

Starting with the G61%/100mm bundle, Fig. 11a and b present the simulated and experimental velocity profiles for this bundle with 50 and 245 lpm, respectively. The velocity profiles in less blocked sub-channels, i.e. B and D, are very similar: the axial velocity increased upstream of the balloon because of the flow redistribution from blocked sub-channels (like A), the axial velocity was almost stable in the ballooned zone, and there was a slight decrease downstream of the balloon. DRACCAR succeeded to estimate their velocity profiles within the experimental uncertainty ($V_{z,n} = \pm 0.1$). For the most blocked sub-channel (A), the axial velocity decreased up- and downstream of

the ballooned zone because of the flow redistribution in the first transition zone and the flow passage area expansion in the second transition zone, as described in detail by Oliveira et al. [18]. In this case, DRACCAR calculated the same velocity profile observed in the experiments but the quantitative results were only accurate in the first transition for 50 lpm and the ballooned zone for both flow rates. Especially downstream of the balloon, DRACCAR overestimated the axial velocity within the blocked sub-channel. This is clearly observed in Fig. 12 where we present the difference between the calculated and experimental $V_{z,n}$ with black horizontal dashed lines to represent the range where DRACCAR calculations are within the experimental uncertainty. We find that DRACCAR results for sub-channel A were fairly accurate except in the second transition zone. Last, for both flow rates, DRACCAR could predict neither qualitatively nor quantitatively the axial velocity profile for sub-channel C, the one neighboring ballooned rods and a guide tube. Although the increase in the first transition zone was well calculated, the decrease in the ballooned zone was not predicted in the simulations, while the decrease in the second transition zone was not as steep as observed in the experimental results (Fig. 11). This difference between simulation and experimental results for sub-channel C is clearer in Fig. 12, especially with 50 lpm since DRACCAR largely overestimated the velocity in these regions.

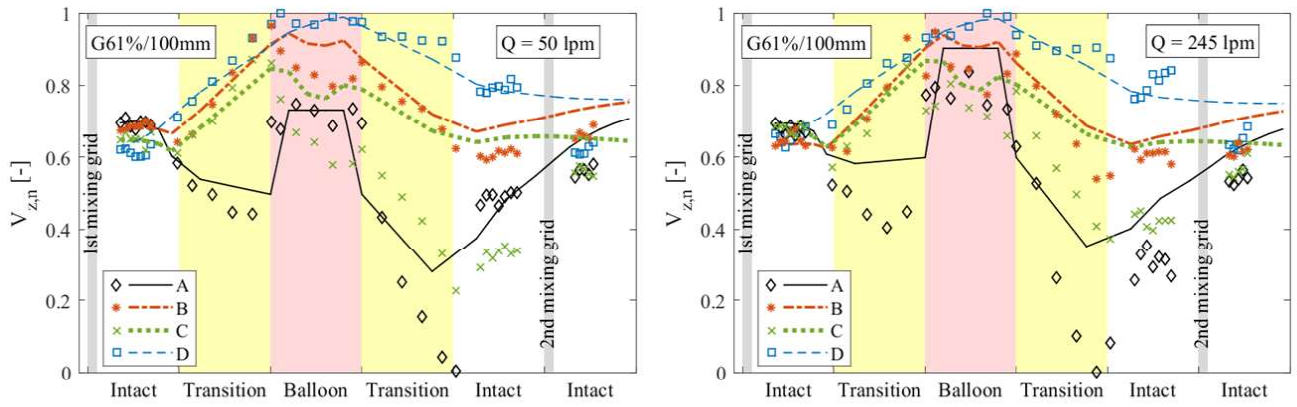

(a) (b)

Figure 11: Normalized velocities (lines are DRACCAR simulations, markers are MASCARA results) in different sub-channels for the G61%/100mm bundle: (a) 50 lpm, and (b) 245 lpm.

Figure 13 presents the DRACCAR and MASCARA results for the axial velocity along the G90%/240mm bundle, while Fig. 14 shows the difference between simulated and experimental axial velocities, both figures for 50 and 245 lpm. As in the previous case, the velocity in the less blocked sub-channels (B and D) increased in the first transition zone, remained stable in the blocked zone and progressively decreased after the balloon. Likewise, DRACCAR adequately estimated the velocity in these sub-channels within the experimental uncertainty, except in the first transition zone for the sub-channel B with 50 lpm. The fluid velocity in the most blocked sub-channel (A) followed a similar behavior to that described for the G61%/100mm bundle. The only difference is the existence of a local minimum in the transition zone upstream of the balloon where the ballooned rods are in touch (as shown in Fig. 5), as discussed in detail by Oliveira et al. [18]. For this sub-channel, DRACCAR estimated quite precisely the axial velocity, being more accurate in the first transition for the two studied flow rates and less accurate at the end of the

second transition zone, underestimating the axial velocity and finding the minimum slightly earlier than MASCARA results. Finally, DRACCAR overestimated the axial velocity for the sub-channel C with the G90%/240mm bundle as we observed with G61%/100mm. Nevertheless, most of the points are within the experimental uncertainty of $V_{z,n} = \pm 0.1$ (Fig. 14).

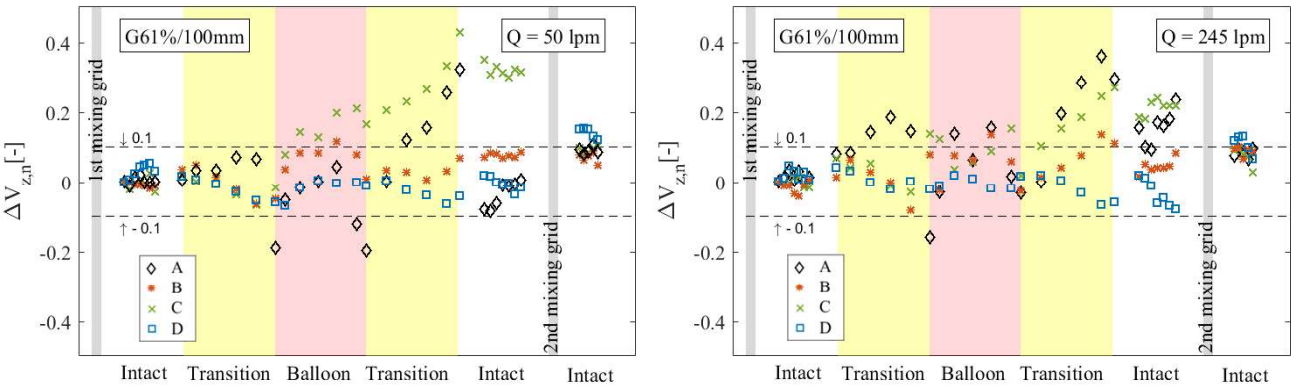

(a) (b)

Figure 12: Difference between simulated (DRACCAR) and experimental (MASCARA) normalized axial velocity for the G61%/100mm bundle

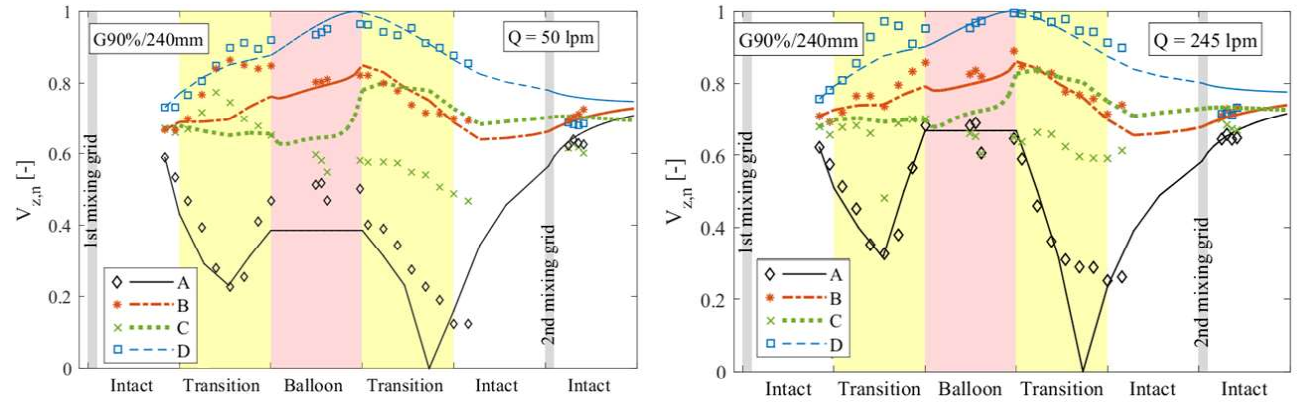

(a) (b)

Figure 13: Normalized velocities (lines are DRACCAR simulations, markers are MASCARA results) in different sub-channels for the G90%/240mm bundle: (a) 50 lpm, and (b) 245 lpm.

Although MASCARA experiments may appear relatively simple for a computational fluid dynamics simulation, we should remind that DRACCAR calculations rely on models with one element containing a whole sub-channel, without detailing the fluid dynamics within. Therefore, modeling the Navier-Stokes equation becomes more complicated, especially the convective term $(V.\nabla V)$ in the Lagrangian derivative. This term is significant in the transition zones, where, in fact, DRACCAR was less accurate (see Figs.12 and Figs. 14). Although the axial velocity estimates for sub-channel C all along with the bundle and sub-channel A in the second transition zone were less accurate, with deviations higher than the experimental uncertainty, DRACCAR succeeded to calculate precisely most of the

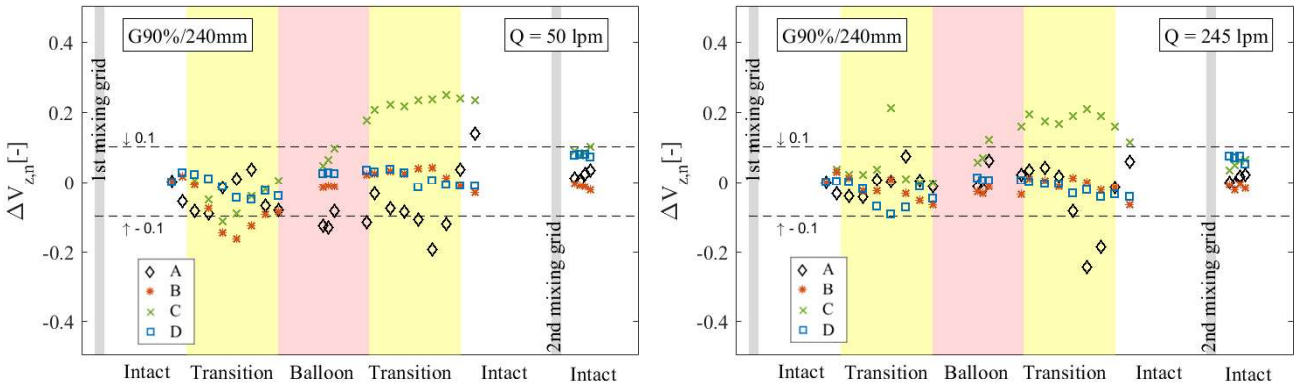

(a) (b)

Figure 14: Difference between simulated (DRACCAR) and experimental (MASCARA) normalized axial velocity for the G90%/240mm bundle

velocity points. Table 2 presents the percentage of axial velocity points that DRACCAR could estimate within the experimental uncertainty for each bundle, flow rate and sub-channel. As we discussed, the calculations for the sub-channel A, the one in the center of the balloon, were in general quite accurate. While DRACCAR was less accurate for this sub-channel with the G61%/100mm bundle and 245 lpm flow rate, it presented a remarkable performance for the G90%/240mm, which is considered one of the most critical scenarios [22]. For less blocked sub-channels, namely B and D, DRACCAR estimated more than 85% of the local axial velocities correctly. As already mentioned, the calculations for sub-channel C (partially blocked by the neighboring balloon and a guide tube) were not accurate enough, which deserves more attention to improve the model in this case, even though this sub-channel is not considered critical as the axial velocity is not much reduced because of the flow redistribution. A more precise analysis of the transverse velocities may help to explain this difference between calculation and experimental data.

Table 2: Percentage of points estimated by DRACCAR within the experimental uncertainty ($V_{z,n} = \pm 0.1$).

	G61%/100mm		G90%/240mm	
Flow (lpm)	50	245	50	245
Sub-channel A	78%	56%	72%	92%
Sub-channel B	97%	89%	88%	100%
Sub-channel C	50%	58%	56%	56%
Sub-channel D	86%	92%	100%	100%
Total points	78%	74%	79%	87%

With the present results, the fluid dynamics model implemented in DRACCAR was validated, especially because of its accurate results for the most blocked sub-channel. Since its heat transfer models were separately validated in a previous study [10], the final step in the thermal-hydraulics axis in project PERFROI will be comparing DRACCAR

simulations with the test results from COAL experiments.

5. Conclusions

In this study, we validated the IRSN DRACCAR LOCA code by comparing the simulations with test results from the MASCARA experimental campaign for two ballooned 7 x 7 bundles with different blockage ratios and lengths (bundles G61%/100mm G90%/240mm) and with different flow rates, one in laminar regime (50 lpm) and the other in turbulent regime (245 lpm). The results showed that DRACCAR succeeded to estimate the axial flow velocity in intact and less blocked sub-channels for both configurations and flow rates. For the blocked sub-channel in the center of the balloon, DRACCAR performed better with the more blocked bundle (G90%/240mm), which is considered one of the worst-case scenarios of clad ballooning during a LOCA. However, for this bundle, the axial flow velocity within this sub-channel was underestimated at the end of the transition zone downstream of the balloon. For the G61%/100mm bundle, DRACCAR succeeds to correctly estimate the velocity profile for this blocked sub-channel and most of the points were estimated within the experimental uncertainty; however, the axial velocity was largely overestimated at the end of the second transition zone. Finally, for the partially-blocked sub-channel neighboring the balloon and a guide tube, the axial velocity estimate deserves more attention to improve its calculation, even though this is not considered a critical sub-channel during a LOCA.

Once COAL experimental campaign will be finished, simulations of the experiments will be performed with DRACCAR including all the involved thermal-hydraulics phenomena during the reflooding phase, which will be an important step for the validation of code. Furthermore, DRACCAR simulations of MASCARA experiments with non-coplanar balloons are also expected, in which balloons are located in different axial positions so the flow redistribution behaves differently from those presented in this study.

6. Acknowledgement

The authors would like to thank Didier Stemmelen, Research Fellow at CNRS and LEMTA (Université de Lorraine), for reviewing this paper and giving valuable suggestions to improve its quality, especially concerning the method and result presentations.

7. Funding

This work is completed within the framework of RSNR Project PERFROI from a French State aid managed by the French National Research Agency under the program of Investments for the Future carrying the reference n° ANR-11-RSNR-0017.

References

[1] G. Repetto, C. Dominguez, B. Durville, S. Carnemolla, D. Campello, C. Tardif, M. Gradeck, The R&D PERFROI project on thermal mechanical and thermal hydraulics behaviors of a fuel rod assembly during a loss of coolant accident, 16th International Topical Meeting on Nuclear Reactor Thermal Hydraulics (NURETH-16) 1 (2015) 1–14.

[2] Y. Jin, F. R. Beck, B. R. Lowery, D. J. Miller, F. B. Cheung, S. M. Bajorek, K. Tien, C. L. Hoxie, Experimental study of droplet sizes across a spacer grid location under various reflood conditions, Experimental Thermal and Fluid Science 94 (February 2017) (2018) 246–257. doi:10.1016/j.expthermflusci.2018.02.017.

[3] H. K. Cho, K. Y. Choi, S. Cho, C.-H. Song, Experimental observation of the droplet size change across a wet grid spacer in a 6x6 rod bundle, Nuclear Engineering and Design 241 (12) (2011) 4649 – 4656, the18th International Conference on Nuclear Engineering (ICONE-18). doi:https://doi.org/10.1016/j.nucengdes.2011.03.042.

[4] Y. Jin, F.-B. Cheung, K. Shirvan, S. M. Bajorek, K. Tien, C. L. Hoxie, Development of a droplet breakup model for dry spacer grid in the dispersed flow film boiling regime during reflood transients, International Journal of Heat and Mass Transfer 143 (2019) 118544. doi:https://doi.org/10.1016/j.ijheatmasstransfer.2019.118544.

[5] J. M. Yoo, B. J. Yun, H. Y. Yoon, J. J. Jeong, Modeling of the droplet entrainment rate in the post-dryout regime for the analysis of a reflood phase, Annals of Nuclear Energy 148 (2020) 107757. doi:https://doi.org/10.1016/j.anucene.2020.107757.

[6] J. Peña Carrillo, A. V. S. Oliveira, A. Labergue, T. Glantz, M. Gradeck, Experimental thermal hydraulics study of the blockage ratio effect during the cooling of a vertical tube with an internal steam-droplets flow, International Journal of Heat and Mass Transfer 140 (2019) 648 – 659. doi:https://doi.org/10.1016/j.ijheatmasstransfer.2019.06.012.

[7] A. V. S. Oliveira, J. D. Peña Carrillo, A. Labergue, T. Glantz, M. Gradeck, Experimental study of dispersed flow film boiling at sub-channel scale in LOCA conditions: Influence of the steam flow rate and residual power, Applied Thermal Engineering 172 (2020) 115143. doi:https://doi.org/10.1016/j.applthermaleng.2020.115143.

[8] N. H. Nguyen, J. Kim, S.-H. Hong, S.-K. Moon, C.-H. Song, Improvements of cobra-tf on the effect of flow blockage during a lb loca with consideration of fuel relocation phenomenon, Nuclear Engineering and Design 325 (2017) 218 – 231. doi:https://doi.org/10.1016/j.nucengdes.2017.08.015.

[9] P. Ruyer, N. Seiler, B. Biton, F. Lelong, F. Secondi, D. Baalbaki, M. Gradeck, Two-phase flow across a partially damaged core during the reflood phase of a LOCA, Nuclear Engineering and Design 264 (2013) 187 – 194, SI:NURETH-14. doi:https://doi.org/10.1016/j.nucengdes.2013.02.026.

[10] A. V. S. Oliveira, J. D. Peña Carrillo, A. Labergue, T. Glantz, M. Gradeck, Mechanistic modeling of the thermal-hydraulics in polydispersed flow film boiling in LOCA conditions, Nuclear Engineering and Design 357 (2020) 110388. doi:https://doi.org/10.1016/j.nucengdes.2019.110388.

[11] Y. Guo, K. Mishima, A non-equilibrium mechanistic heat transfer model for post-dryout dispersed flow regime, Experimental Thermal and Fluid Science 26 (6-7) (2002) 861–869. doi:10.1016/S0894-1777(02)00195-4.

[12] C.-H. Song, Some issues and challenges in advanced thermal-hydraulic safety research, Nuclear Technology 196 (3) (2016) 421–445. doi:https://doi.org/10.13182/NT16-91.

[13] G. Repetto, T. Glantz, G. Guillard, B. Bruyère, Q. Grando, Core coolability in loss of coolant accident: the COAL experiments investigating the thermal hydraulics of a rod bundle with blocked area during the reflooding, 17th International Topical Meeting on Nuclear Reactor Thermal Hydraulics (NURETH-17) 1 (2017) 359–372.

[14] G. Repetto, C. Marquié, B. Bruyère, T. Glantz, Core coolability in loss of coolant accident: the COAL experiments, 16th International Topical Meeting on Nuclear Reactor Thermal Hydraulics (NURETH-16) 1 (2015) 24–37.

[15] S. Bascou, O. De Luze, S. Ederli, G. Guillard, Development and validation of the multi-physics DRACCAR code, Annals of Nuclear Energy 84 (2015) 1–18. doi:10.1016/j.anucene.2014.09.040.

[16] T. Glantz, T. Taurines, O. De Luze, S. Belon, G. Guillard, F. Jacq, DRACCAR: A multi-physics code for computational analysis of multi-rod ballooning, coolability and fuel relocation during LOCA transients Part one: General modeling description, Nuclear Engineering and Design 339 (June) (2018) 269–285. doi:10.1016/j.nucengdes.2018.06.022.

[17] T. Glantz, T. Taurines, S. Belon, O. De Luze, G. Guillard, F. Jacq, DRACCAR: A multi-physics code for computational analysis of multi-rod ballooning, coolability and fuel relocation during LOCA transients. Part Two: Overview of modeling capabilities for LOCA, Nuclear Engineering and Design 339 (August) (2018) 202–214. doi:10.1016/j.nucengdes.2018.08.031.

[18] A. V. S. Oliveira, D. Stemmelen, S. Leclerc, T. Glantz, A. Labergue, G. Repetto, M. Gradeck, Parametric effects on the flow redistribution in ballooned bundles evaluated by magnetic resonance velocimetry, Experimental Thermal and Fluid Science 125 (2021) 110383. doi:https://doi.org/10.1016/j.expthermflusci.2021.110383.

[19] A. V. S. Oliveira, D. Stemmelen, S. Leclerc, T. Glantz, A. Labergue, G. Repetto, M. Gradeck, Velocity field and flow redistribution in a ballooned 7×7 fuel bundle measured by magnetic resonance velocimetry, Nuclear Engineering and Design 369 (2020) 110828. doi:https://doi.org/10.1016/j.nucengdes.2020.110828.

[20] P. Chatelard, S. Belon, L. Bosland, L. Carénini, O. Coindreau, F. Cousin, C. Marchetto, H. Nowack, L. Piar, L. Chailan, Main modelling features of the astec v2.1 major version, Annals of Nuclear Energy 93 (2016) 83–93, eRMSAR-2015 conference of SARNET in the frame of the NUGENIA Technical Area 2. doi:https://doi.org/10.1016/j.anucene.2015.12.026.

[21] P. Emonot, A. Souyri, J. Gandrille, F. Barré, Cathare-3: A new system code for thermal-hydraulics in the context of the neptune project, Nuclear Engineering and Design 241 (11) (2011) 4476–4481, 13th International Topical Meeting on Nuclear Reactor Thermal Hydraulics (NURETH-13). doi:https://doi.org/10.1016/j.nucengdes.2011.04.049.

[22] C. Grandjean, Coolability of blocked regions in a rod bundle after ballooning under LOCA conditions: Main findings from a review of past experimental programmes, Nuclear Engineering and Design 237 (15) (2007) 1872 – 1886, NURETH-11. doi:https://doi.org/10.1016/j.nucengdes.2007.02.022.

[23] I. Idel'cik, Mémento des pertes de charges, 3rd Edition, Eyrolles, EDF, Paris, 1986.

Simulation of flow redistribution in 7x7 ballooned fuel bundle experiments using DRACCAR code

J.E. Luna Valencia[a,b], A.V.S. Oliveira[b], T. Glantz[a], A. Labergue[b], S. Leclerc[b], M. Gradeck[b,*]

[a] *IRSN, PSN, B.P. 3, 13115 Saint Paul-Lez-Durance, France*
[b] *Université de Lorraine, CNRS, LEMTA, F-54000 Nancy, France*

Abstract

IRSN has developed DRACCAR code in order to model loss of coolant accidents (LOCA) in a light water nuclear reactor. The physics during a hypothetical loss of coolant accident involves several phenomena such as heat and mass transfers, fluid dynamics, mechanics, and chemistry. Even if the modeling requires these conjugated processes, it is important to validate them separately first. Clad ballooning can occur during a LOCA, leading to flow redistribution between sub-channels. In this paper, we present DRACCAR simulations of the fluid dynamics in two 7 x 7 ballooned bundles with different blockage ratios and ballooned lengths and with two different flow rates, one laminar and the other turbulent. DRACCAR results for the axial velocities in specific sub-channels are compared to experimental data obtained by MRI techniques on the MASCARA facility. The present results show that in most of the sub-channels studied, DRACCAR is capable of predicting correctly the velocity profiles for both bundles and flow rates. The axial velocity is, in general, well estimated by DRACCAR, especially for the intact and less-blocked sub-channels. For the most blocked subchannel, DRACCAR is able to estimate the majority of the axial velocity in a margin of ±15% with respect to the MASCARA values, except for the most blocked subchannel in laminar flow.

Keywords:

LOCA, Nuclear reactor, Clad ballooning, Thermal-hydraulics, Reflooding, Magnetic Resonance Imaging

1. Nomenclature

Latin letters

d	Nuclear rod diameter
L_b	Blocked length
k	Pressure drop coefficient
p	Nuclear rod pitch
S_b	Blocked sub-channel flow passage area
S_0	Intact sub-channel flow passage area
V	Velocity
V_{min}	MASCARA's minimum axial velocity
V_{max}	MASCARA's maximum axial velocity
$\widetilde{V}_{ref}$	Bulk mean velocity
V_z	Axial velocity
$V_{z,n}$	Normalized axial velocity
z	Axial distance

Greek letters

τ_b	Dimensionless blockage ratio

*Corresponding author
Email address: michel.gradeck@univ-lorraine.fr (M. Gradeck)

2. Introduction

One hypothetical accident that is considered for the design of the safety systems of pressurized-water reactors (PWR) is the Loss of Coolant Accident, commonly referred to as LOCA. During the course of such an accident, the fuel rods heat dissipation can be highly degraded and the fuel assemblies' temperature rapidly increases. In some cases, it leads to the ballooning or burst of some of the pressurized fuel rods and the formation of blocked sub-channels (Fig. 1) [1]. The emergency core cooling system (ECCS) is designed to inject fresh water into the nuclear reactor's core to impede the fuel assemblies to reach prohibitive temperatures. This step is known as the reflooding phase. Because of the high temperature of the fuel rods, the injected water partially evaporates and a steam-droplet two-phase flow is created downstream of the water level. This phenomenon plays a very important role in the coolability of the regions not yet immersed in water.

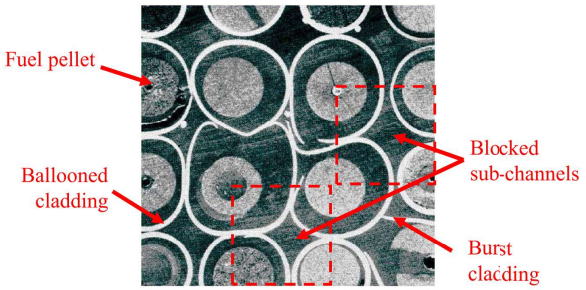

Figure 1: Picture after PHEBUS in-pile LOCA experiment showing the clad ballooning and the formation of blocked sub-channels [1].

Different thermal-hydraulic studies have been carried out to characterize this two-phase flow and its cooling capacity: the droplets' size across spacer grids under reflood conditions [2, 3], the modeling of droplets breakup and entrainment during the reflooding phase [4, 5] and the droplets dynamics and heat transfer between the flow and the nuclear rods at sub-channel scale [6, 7]. Furthermore, the steam flow rate entering the blocked sub-channels is decreased due to its preferential deviation to less deformed sub-channels [8]. Ruyer et al. [9] observed in a CFD analysis that with this steam deviation, the large droplets tend to continue their path toward the blocked sub-channel because of their high inertia. Nevertheless, this is still particularly critical because heat transfer due to wall-to-steam convection is highly decreased in blocked sub-channels, as this is the most important heat dissipation process during a LOCA [10, 11]. For this reason, the thermal-hydraulics in blocked sub-channels raises concerns on the core coolability to guarantee nuclear safety [12].

In order to increase the knowledge on the cooling of a reactor's core during a LOCA, the French Institut de Radioprotection et de Sûreté Nucléaire (IRSN) launched the PERFROI project intending to perform high-quality experiments for better understanding the thermal-hydraulic and thermomechanic behaviors of the damaged core during a LOCA. In the thermal-hydraulics axis, the main experiment (named COAL[1] [13, 14]) consists of a bundle of electrically heated rods, with the blockage region simulating clad ballooning and fuel relocation (balloons filling up with fuel pellets, associated with a possible power profile modification [15–17]), using a 7 x 7 bundle geometry at full-length scale. The test section instrumentation counts with many thermocouples placed on the sheaths, on the housing

[1] COAL: **CO**olability of a fuel **A**ssembly during **L**OCA

and in the flow. Although COAL experiments allow the thermal-hydraulics characterization during the reflooding phase, information on the heat transfer and fluid dynamics processes is hidden in this large-scale experiment. For this reason, additional experimental campaigns were carried out to complement COAL with information on the two-phase flow heat transfer and hydraulics. On the one hand, experiments with COLIBRI[2] experimental apparatus [6, 7] resulted in a precise characterization of the heat transfer phenomena by analyzing a steam-droplets flow within a vertical tube in LOCA conditions at the sub-channel scale. On the other hand, using MRI techniques, the experimental campaign MASCARA[3] [18, 19] provided valuable information on the flow redistribution in the presence of ballooned zone within several 7 x 7 bundles. The geometries tested in MASCARA were very similar to the test sections that will be used in COAL experiments. Therefore, while COLIBRI contributed to the analysis of the thermal phenomena and the droplets dynamics, MASCARA campaign isolated the hydraulics from thermal effects and analyzed the flow behavior when passing through spacer grids and ballooned fuel rods.

All the effort spent in experimental campaigns is justified because they serve to acquire knowledge of the involved physical phenomena and integrate it into computer codes such as DRACCAR[4], an IRSN's code that describes the 3D thermomechanical behavior and reflooding of a fuel assembly including its coolability as well as its embrittlement during a LOCA. The code evaluates the blockage ratio associated with deformed fuel rods and their impact on core cooling. Also, DRACCAR simulates the uncovery (dewatering) phase of cooling accidents affecting spent fuel pools. This calculation implies complex computations involving multi-phase flow, coupled with heat transfers, chemical reactions, mechanical strain, and fuel relocation. To accomplish this, DRACCAR combines two codes, one for the thermomechanical and chemical behavior calculation of the fuel assemblies and the second one, for the thermal-hydraulics behavior calculation for the flow that passes through these assemblies [16, 17]. In thermal-hydraulics simulations, DRACCAR is coupled to two different thermal-hydraulic codes, CESAR [20] and CATHARE-3 [21].

DRACCAR simulations of COLIBRI experiments have already been performed [10] and very good agreement has been observed, even though the heat transfer by droplets impact onto the heated wall has been neglected – this heat transfer phenomenon can contribute up to 10% to the internal heat dissipation (for an intact tube and a droplet volume fraction of about 10^{-4}), as evaluated by Peña Carrillo et al. [22]. The next step, before the simulation of COAL experiments with DRACCAR, is the simulation of the MASCARA hydraulics experiments, object of the present paper. Although Oliveira et al. tested several geometries and flow rates [18, 19], we compare herein calculations and experimental results for two flow rates and two bundles: one bundle with 90% of blockage ratio and 240 mm of blockage length and one with 61% of blockage ratio and 100 mm of blockage length, both with flow rates of 50 and 245 lpm. In this study, the DRACCAR/CATHARE-3 coupling is used in the simulations.

3. MASCARA: experimental apparatus and procedure

MASCARA device has been developed to measure three-component velocity fields in fuel rods bundles having ballooned zones using magnetic resonance velocimetry (MRV). More than 1,000 velocity fields were obtained with seven different bundles and four different flow rates, some results were presented in detail in previous studies, like

[2]COLIBRI: **CO**o**LI**ng of **B**lockage **R**egion **I**nside a PWR Reactor
[3]MASCARA: **M**RI of **A**ssembly **S**ub-**C**hannels for the **A**nalysis of **R**eactor **A**ccidents.
[4]DRACCAR: **D**éformation et **R**enoyage d'un **A**ssemblage de **C**rayons **C**ombustibles pendant un **A**ccident de **R**efroidissement

comparing the flow in an intact bundle and a ballooned one [19] and analyzing parametric effects on the flow redistribution because of clad ballooning [18]. Detailed information regarding the measurement techniques, the MRV sequence and parameters, data reduction and uncertainties are available in these previous works. In this paper, we present only the main aspects concerning the test section that are important when comparing the experimental results with DRACCAR simulations.

MASCARA's experimental bench is schematically represented in Fig. 2, consisting of a regular single-phase hydraulic circuit with a screw pump connected to a damper in order to assure a stable flow in all the circuit, pressures transducers for safety purposes, an electromagnetic flowmeter to measure the water flow rate, which is later used for validating the MRV measurements (comparing the flowmeter value with the calculated flow rate using MRV results), and the test section, which is placed horizontally. This one consists of a 7 x 7 representative test bundle, which is inserted into a radiofrequency (RF) coil and this assembly is, in turn, inserted into the MRI scanner. The intact rods were made of polycarbonate tubes, while the ballooned rods were constructed by 3D printing (FDM - fused deposition modeling) using PLA as the base polymer. Furthermore, the four spacer grids were made of Inconel and they had the same material and geometry used in COAL experiments (Fig. 3)[1]. These grids were not made of a ferromagnetic material; however, they still disturbed the magnetic field and impeded accurate velocity field measurements by 4 cm close to them.

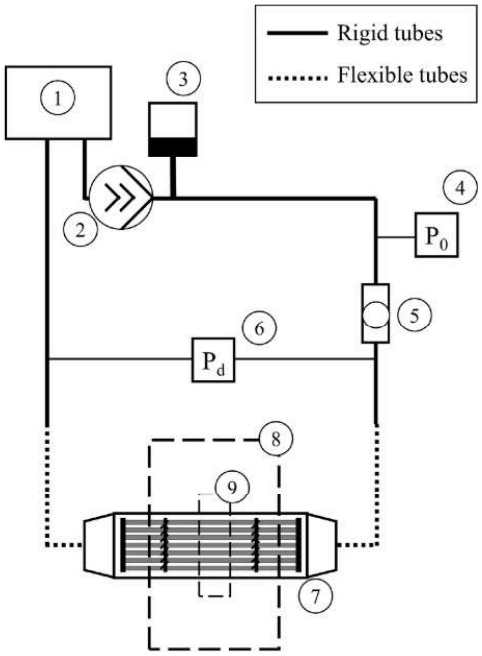

Figure 2: Hydraulic circuit of MASCARA: 1) water tank, 2) eccentric screw pump, 3) damper, 4) absolute pressure transducer, 5) electromagnetic flowmeter, 6) differential pressure transducer, 7) test section, 8) MRI scanner, 9) radio- frequency (RF) coil. ([19]).

All the bundles tested by Oliveira et al. [18] had 49 elements arranged in a 7 × 7 structure, having thirty tubes with 9.5 mm diameter to represent intact fuel rods, sixteen ballooned tubes, and three tubes with a 12.45 mm diameter to represent guide tubes. In this study, we chose two bundles having two different blockage ratios and two different blockage lengths, named G61%/100mm and G90%/240mm, to compare with DRACCAR simulations. The

blockage ratio τ_b describes the reduction in the cross-sectional area because of the cladding ballooning and is defined by:

$$\tau_b = 1 - \frac{S_b}{S_0} \tag{1}$$

where S_b and S_0 are the flow passage areas of a blocked and an intact sub-channel, respectively. The first bundle, G61%/100mm, represents the case where the blocked sub-channels are formed by four ballooned rods that touch their neighboring rods without losing the circular shape ($\tau_b = 61\%$ in Fig. 4), with a blockage length of 100 mm. The second bundle, G90%/240mm, represents a severe blockage ratio and length, as mentioned by Grandjean [23]. In this case, the blocked sub-channels are formed by ballooned fuel rods with a squared shape and rounded corners, due to joint deformation with neighboring rods ($\tau_b = 90\%$ in Fig. 4). Therefore, in the ballooned zone (for τ_b equal to both 61% and 90%), the flow within blocked sub-channels is isolated from neighborhood sub-channels.

Figure 3 shows the side view of these two test section configurations and the position of the spacer grids and the ballooned zone, with their values given in Table 1. The first and the last spacer grids do not have mixing vanes, while the two in the middle have mixing vanes with remarkable performance to homogenize the flow, as described in previous studies [19]. The distance of 522 mm between the two mixing spacer grids in the middle (E – A) was fixed because it is approximately the same distance found in typical French PWR's. Figure 4, in turn, shows the bundles cross-sectional views in the intact and ballooned zones, the first only having intact sub-channels (no ballooning) and the second having the balloons whose shape corresponds to the bundles blockage ratios (61% and 90%).

Table 1: Dimensions of the tested bundles as shown in Fig. 3 (in mm).

Bundle	τ_b	L_b	A	B	C	D	E	F	E-A
G61%/100mm	61%	100	252	444[a]	479	614[a]	774	1073	522
G90%/240mm	90%	240	282	370	435	740	803	1072	521

[a] In our previous study [18], these dimensions were incorrectly presented (difference of 10 mm). These are the correct values.

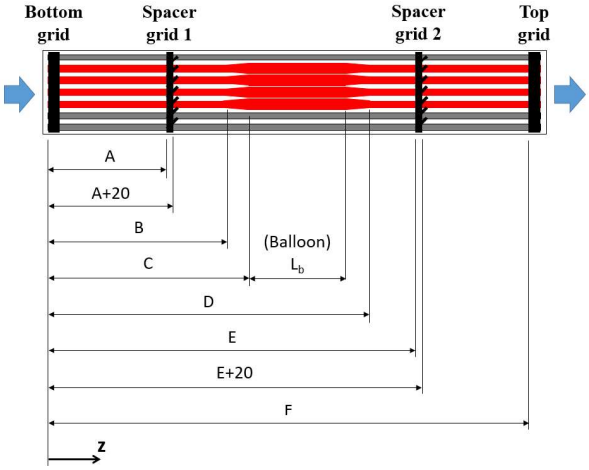

Figure 3: Axial positions of the grids and the balloon in the bundles.

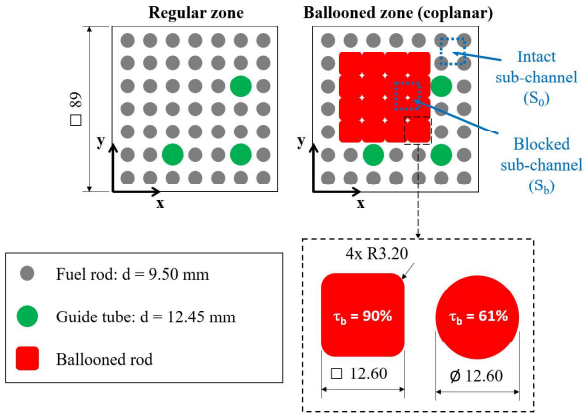

Figure 4: Section view in the intact and ballooned zones, with evidence on the ballooned fuel rods' shapes for 61% and 90% blockage ratios ([19]).

Between the intact and the ballooned regions, there is a transition zone (Fig. 5). For the G61%/100mm bundle with a blockage ratio of 61%, the fuel rods cross-section increases keeping the circular shape and the transition finishes where they are in contact. The length of this transition is 35 mm. For the case of the G90%/240mm bundle with a 90% blockage ratio, there is a first transition like the one in the G61%/100mm bundle and a second transition zone, which is 30 mm long, where the fuel rods shape continues deforming progressively until reaching the final cross-section shown in Fig. 4. For both bundles, there is another transition zone downstream of the balloon, exactly like the first but mirrored.

As mentioned at the beginning of this section, MRV was the technique we used to measure the velocity fields in these bundles. We used a typical gradient-echo pulse sequence with an additional flow encoding sequence, as explained by Oliveira et al. [19]. The pixel resolution was 0.47 x 0.47 mm^2 and the experimental procedure ensured the velocity uncertainty in one pixel to be about $\pm 20\%$ of the bulk mean velocity [19]. However, to compare the experimental results with DRACCAR simulations, we must take the mean axial velocity within a sub-channel. In this case, the uncertainty of this mean velocity is reduced to $\pm 10\%$ of the flow mean velocity, as discussed by Oliveira et al. [18].

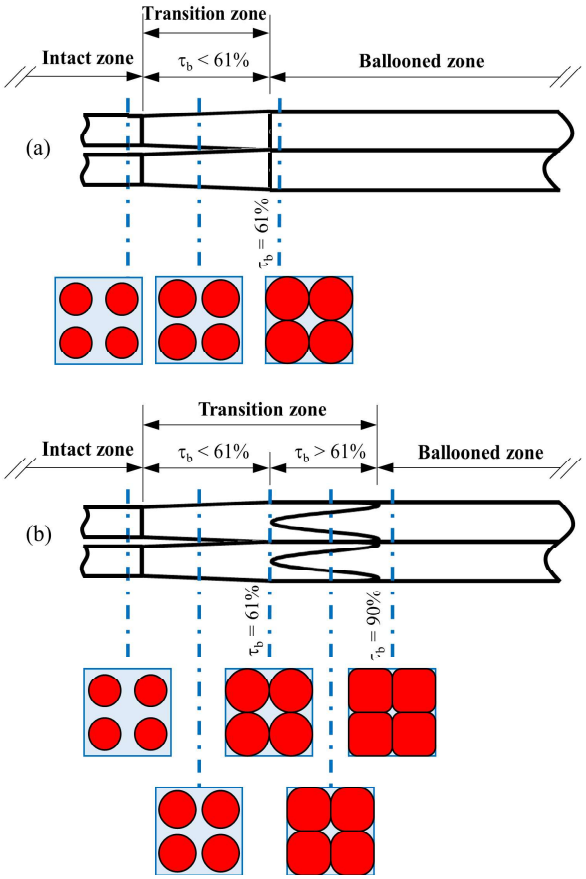

Figure 5: Transition from regular to ballooned zone for both bundles: a) G61%/100 mm; b) G90%/240mm.

4. DRACCAR: details of the simulation

4.1. Modeling concept

DRACCAR is a code from the FUEL+ software platform developed by IRSN since 2008 to simulate the 3D thermo-mechanical deformation and the reflooding of fuel rods during a LOCA (among other phenomena). DRACCAR allows modeling problems with different scales, from a single fuel rod or fuel assembly to the entire reactor's core or spent fuel pool. Moreover, this code can perform calculations including fuel assembly components like control rods, fuel rods (modeling both the stack of fuel pellets and the cladding), instrumentation tubes, guide tubes, and spacer grids. To achieve this, DRACCAR couples two codes: a thermo-mechanical code ICARE3D and one of the two different thermal-hydraulic codes, CESAR and CATHARE-3 [16]. In the present study, we coupled DRACCAR with CATHARE-3 and disabled the thermo-mechanical package as it was unnecessary to simulate MASCARA experiments.

The CATHARE code is the result of a joint project of CEA (Research and Development institute), EDF (operator and electricity supplier), FRAMATOME (Power plant designer), and IRSN (technical support of French Safety Authority) aiming to develop and provide a thermal-hydraulics system code in support of the French nuclear fleet. CATHARE has been intensively used for the French nuclear fleet (plant or component design, safety studies, normal and emergency procedures validation, uncertainties analysis, etc.), and largely and internationally distributed among research institutes. The code is developed and maintained at CEA, by the CATHARE team.

CATHARE is modular code where several modules can be connected to represent any hydraulic circuit. The three main hydraulic modules are:

- the 1-D module to describe pipes,
- the 0-D module to describe large capacities,
- the 3-D module to describe multidimensional effects in specific components.

All these modules use by default a 2-phase model to describe steam-liquid flows and four non-condensable gases can be transported. Both thermal and mechanical non-equilibrium of the two phases is described thanks to the 3 balance equations solved for each phase: mass, momentum, and energy. All kinds of two-phase flow patterns are modeled, in laminar and turbulent regimes.

The numerical method in CATHARE code uses a first-order finite volume - finite difference scheme with a staggered mesh and the donor cell principle. The time discretization varies from the fully implicit discretization used in the 0-D and 1-D modules to the semi-implicit scheme used in the 3-D module [24].

4.2. Simulation domain and conditions

The DRACCAR calculations of MASCARA experiments aim reproducing the fluid dynamic upstream, within and downstream of the ballooned zone; that is why the modeling domain is restricted to the bundle part downstream the first mixing grid. Moreover, the DRACCAR models associated to grids are not detailed enough to precisely reproduce the impact of the mixing vanes on the fluid as observed in the experiments, leading to a calculated fluid flow distribution slightly different from the experimental one. In order to overcome this problem, it has been chosen to match the inlet of the domain to the first position after the mixing grid where MRV measurements were performed and to impose the experimental results as inlet boundary conditions (that is to say the axial fluid velocity at the inlet of each sub-channel). The end of the modeling domain corresponds to the end of the MASCARA bundle. The second grid is only simulated through the use of a singular pressure drop coefficient. At the outlet of each sub-channel, a pressure boundary condition is defined, and the outlet pressure value is set to the atmospheric pressure (Fig. 6).

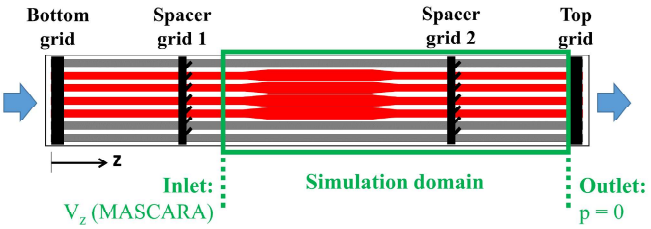

Figure 6: Simulation domain of the present study.

As transverse flow is expected in MASCARA, the 3D module of CATHARE is used for the simulation, so a 3D structured mesh with hexahedral elements is considered. Considering a transverse plane (i.e. a cross-sectional cut), each element contains only one sub-channel, which means that DRACCAR does not calculate velocity within the sub-channel. Figure 7 presents an axial cut at $z = 142mm$ with the G90%/240mm bundle, showing the mesh used in MASCARA simulation, which contains 64 sub-channels to model a whole MASCARA bundle. The sub-channels are

as well meshed in the axial direction. The axial discretization is the same for all the sub-channels and depends on the bundle considered: for the G61%100mm bundle, we used 24 axial elements, of which 8 correspond to the transition and ballooned zones (in total 64 x 24 = 1536 fluid meshes are used for this bundle). For the G90%/240mm bundle, we used 41 axial elements, 14 of them being in the transition and ballooned zones (in total 2624 fluid meshes are considered).

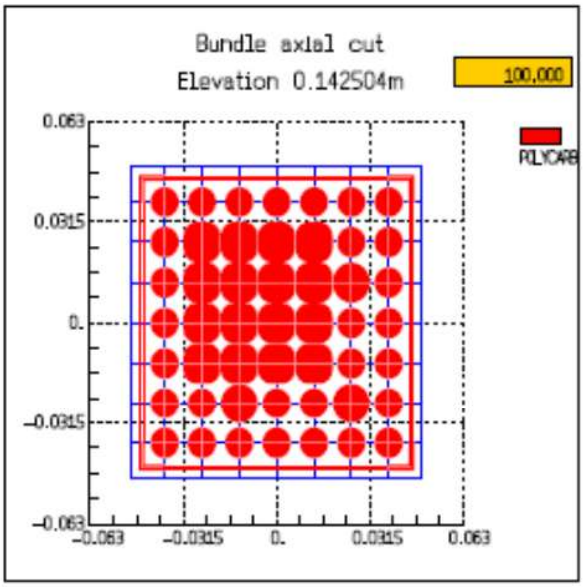

Figure 7: Example of meshing used for MASCARA (the meshing is in blue – the structures are in red) with the G90%/240mm bundle at $z = 142$ mm.

The exact geometries and positions of the 30 intact fuel rods, 3 guide tubes and housing used in MASCARA experiments were simulated with DRACCAR, which means the fluid passage section areas (in all the three directions) and the friction perimeter were as well correctly represented. The axial ballooned rods shape could not be simulated continuously over the axial DRACCAR meshing. Thus, their complex geometry was modeled to preserve the exact fluid passage area and friction perimeter at all the mesh faces (where the momentum balances equations are solved), as shown in Fig. 8. This modeling was performed following several steps. First, we calculated the volume of each ballooned rod forming a given sub-channel. Then, this rod volume was divided by the element dimension in each direction to obtain the wall section area. Finally, this section area was subtracted to the total element section area to obtain the precise fluid section area for the concerned face. With this choice, in the axial direction, the diameter of the tube was precisely equal to 12.6 mm between the two transitions (Fig. 8).

For the axial singular pressure losses, a coefficient equal to 1.38 (k, classical coefficient used for this type of grid) is imposed at the modeled grid elevation. For the radial singular pressure drop, k is calculated using modified Idel'cick equation [25]:

$$k = 0.228 \left(\frac{p}{d} - 1 \right)^{-0.5} \tag{2}$$

where p and d are respectively the pitch and the external rod diameter.

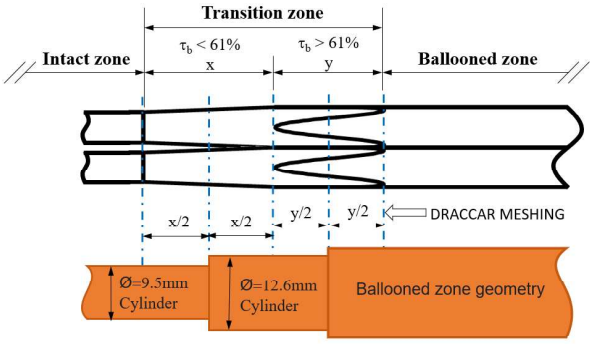

Figure 8: Example of balloon modeling with DRACCAR.

4.3. DRACCAR/MASCARA comparison

Oliveira et al. [19] presented velocity fields like the example in Fig. 9a (without transverse velocities), the colored bar referring to the magnitude of the axial velocity V_z (z-direction, Fig. 6) normalized with the bulk mean velocity $\widetilde{V}_{ref}$. Nevertheless, DRACCAR simulations only provide mean velocities for each sub-channel, i.e. without detailing the velocity field within the sub-channels. Even though DRACCAR calculates transverse velocities, we did not compare these calculations with experimental data because there is a deterministic error in MASCARA measurements of transverse velocities by MRV that could not be corrected [18]. Therefore, only axial velocity results were compared, which is the most important velocity vector in thermal calculations. In addition, MASCARA results of velocity fields were re-processed to obtain the mean axial velocity for each sub-channel. Fig. 9b presents the same velocity field shown in Fig. 9a but now with the normalized mean axial velocity for each sub-channel, which can be compared with DRACCAR simulations. Furthermore, we used two flow rates for the DRACCAR simulation: 50 lpm and 240 lpm, corresponding to a Reynolds number of 1936 and 9599 respectively (laminar and turbulent flow). The flow behavior of these two flow regimes is described by Oliveira et al.[19].

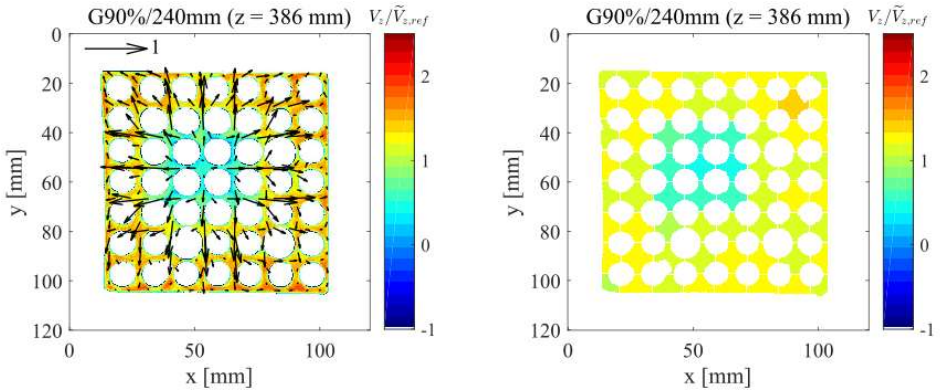

(a) (b)

Figure 9: Example for G90%/240mm bundle at 50 lpm of: (a) a normalized axial velocity field obtained by MRI techniques (MASCARA result, and (b) its corresponding normalized mean axial field for each sub-channel for comparison with DRACCAR simulation, both at $z = 386mm$.

Comparing visually the velocity fields as in Fig. 9 or presenting velocity profiles for all the 64 sub-channels would not be practical nor simple to validate the DRACCAR simulations. Therefore, we chose specific sub-channels to

compare MASCARA and DRACCAR results (Fig. 10), each one with specific blockage and location characteristics as listed below:

- **A**: a sub-channel with the highest blockage ratio, in the center of the ballooned zone ($\tau_{b,A} = \tau_b$ of each bundle);
- **B**: a moderately blocked sub-channel between two intact rods and two ballooned rods ($\tau_{b,B} = 30.6\%$ for G61% and $\tau_{b,B} = 45\%$ for G90%);
- **C**: a moderately blocked sub-channel between one guide tube, one intact rod, and two ballooned rod ($\tau_{b,C} = 45\%$ for G61% and $\tau_{b,C} = 59.5\%$ for G90%);
- **D**: an intact sub-channel ($\tau_{b,D} = 0\%$ for both bundles).

These sub-channels present axial velocity profiles with different behaviors that worth the discussion in this paper. Other sub-channels could also be used in the results presentation, like those partially blocked in the corners of the ballooned zone (for example, the one between D and D' or the sub-channel at two sub-channels above C) or those neighboring the housing. They were not used because the first is less critical than the chosen partially blocked sub-channels and the latter presented practically the same velocity profile of an intact sub-channel.

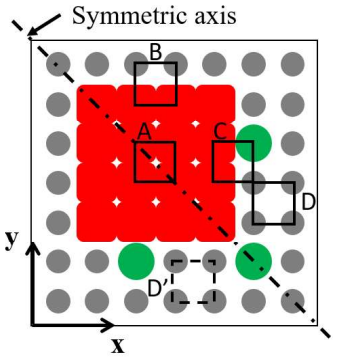

Figure 10: Sub-channels chosen for this study and the bundle symmetry axis, showing an example of symmetric sub-channels (D and D').

The tested geometry was designed to be symmetric to an inclined axis (Fig. 10), which should result in a velocity field as well symmetric to the same axis. However, the bundles used in MASCARA could be slightly misaligned inside the housing [19] and this would favor the axial flow in one sub-channel compared to its symmetric one, although the difference is negligible most of the times. We present examples of this result with the G90%/240mm bundle at the beginning of the results presentation. To reduce experimental biases because of the bundle misalignment and to better validate DRACCAR simulations, we used the mean velocity of the two symmetric sub-channels of MASCARA results. Moreover, averaging the sub-channel velocities reduces the experimental uncertainty because considering more pixels in the averaging population reduces the measurement noise. Figure 10 presents an example of symmetric sub-channels (D and D'), so the experimental results presented in the next section for this sub-channel are actually the average of two symmetrical sub-channels.

5. Results and discussion

We present herein the results as axial velocity profiles for the chosen sub-channels shown in Fig. 10 and for both bundles (G61%/100mm and G90%/240mm) and flow rates (50 and 245 lpm). For a better comparison of MASCARA and DRACCAR results, we normalized both axial positions according to the zone in the bundle and the sub-channels' axial velocities. The first normalization was done by taking the position within a given zone (intact, transition or balloon) and dividing it by the length of this zone. Meanwhile, the axial velocity normalization was performed according to the following equation:

$$V_{z,n} = \frac{V_z - V_{min}}{V_{max} - V_{min}} \tag{3}$$

where V_{min} and V_{max} are, respectively, the minimal and maximal mean axial velocities obtained in MASCARA. We remind that V_z is the mean velocity at each axial position of each sub-channel, either measured in MASCARA or calculated by DRACCAR.

As mentioned in the previous section, we present in Fig. 11 results for symmetric sub-channels with the G90%/240mm bundle for the two tested flow rates. Because DRACCCAR simulations result in perfectly matched axial velocity profiles for symmetric sub-channels, only one of its curves is presented in the figure. For MASCARA results, the axial velocities of symmetric sub-channels are very similar for both flow rates but do not match perfectly, which is natural in experiments. Hence, using average values for MASCARA axial velocities to compare with DRACCAR simulations is reasonable to reduce experimental imperfections, even if they are very small.

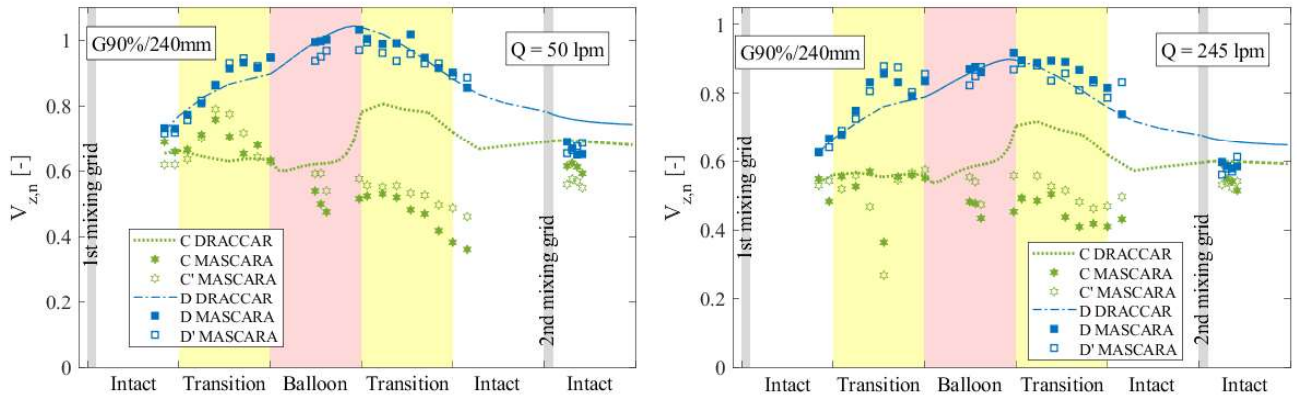

(a) (b)

Figure 11: Comparison of axial profiles in symmetric sub-channels for the G90%/240mm bundle: (a) 50 lpm, and (b) 245 lpm.

Starting with the G61%/100mm bundle, Fig. 12a and b present the simulated and experimental velocity profiles for this bundle with 50 and 245 lpm, respectively. The velocity profiles in less blocked sub-channels, i.e. B and D, are very similar: the axial velocity increased upstream of the balloon because of the flow redistribution from blocked sub-channels (like A), the axial velocity was almost stable in the ballooned zone, and there was a slight decrease downstream of the balloon. DRACCAR succeeded to estimate their velocity profiles within the experimental uncertainty ($\Delta V_{z,n} = \pm 0.09$ for G61%/100mm, 50lpm and $\Delta V_{z,n} = \pm 0.1$ for G61%/100mm, 245lpm). For the most blocked sub-channel (A), the axial velocity decreased up- and downstream of the ballooned zone because of the

flow redistribution in the first transition zone and the flow passage area expansion in the second transition zone, as described in detail by Oliveira et al. [18]. In this case, DRACCAR calculated the same velocity profile observed in the experiments but the quantitative results were only accurate in the first transition for 50 lpm and the ballooned zone for both flow rates. Especially downstream of the balloon, DRACCAR overestimated the axial velocity within the blocked sub-channel. Hence, we find that DRACCAR results for sub-channel A were fairly accurate except in the second transition zone. Last, for both flow rates, DRACCAR could predict neither qualitatively nor quantitatively the axial velocity profile for sub-channel C, the one neighboring ballooned rods and a guide tube. Although the increase in the first transition zone was well calculated, the decrease in the ballooned zone was not predicted in the simulations, while the decrease in the second transition zone was not as steep as observed in the experimental results (Fig. 12).

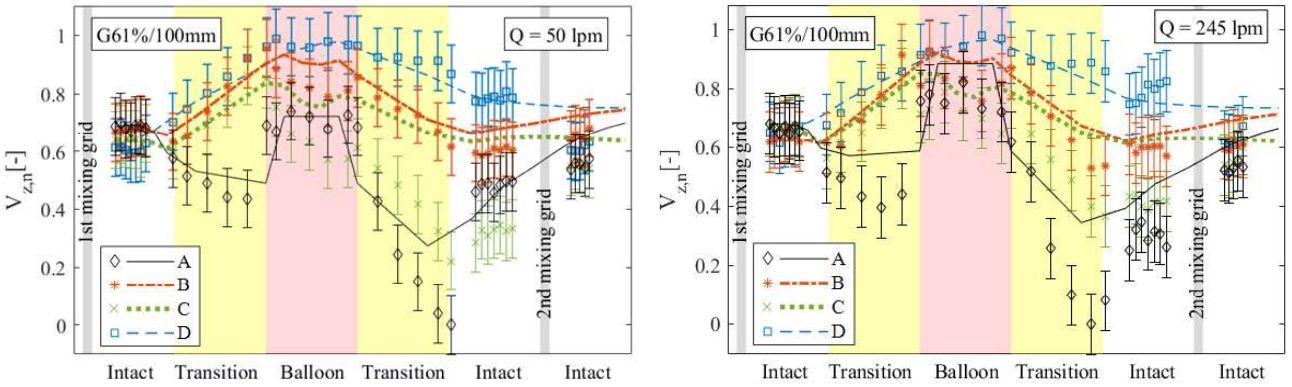

(a) (b)

Figure 12: Normalized velocities (lines are DRACCAR simulations, markers are MASCARA results) in different sub-channels for the G61%/100mm bundle: (a) 50 lpm, and (b) 245 lpm.

Figure 13 presents the DRACCAR and MASCARA results for the axial velocity along the G90%/240mm bundle for 50 and 245 lpm. As in the previous case, the velocity in the less blocked sub-channels (B and D) increased in the first transition zone, remained stable in the blocked zone and progressively decreased after the balloon. Likewise, DRACCAR adequately estimated the velocity in these sub-channels within the experimental uncertainty ($\Delta V_{z,n} = \pm 0.06$ for G90%/240mm, 50lpm and $\Delta V_{z,n} = \pm 0.07$ for G90%/240mm, 245lpm), except in the first transition zone for the sub-channel B with 50 lpm. The fluid velocity in the most blocked sub-channel (A) followed a similar behavior to that described for the G61%/100mm bundle. The only difference is the existence of a local minimum in the transition zone upstream of the balloon where the ballooned rods are in touch (as shown in Fig. 5), as discussed in detail by Oliveira et al. [18]. For this sub-channel and for the higher flow rate, DRACCAR estimated quite precisely the axial velocity, being more accurate in the first transition and less accurate at the end of the second transition zone, underestimating the axial velocity and finding the minimum slightly earlier than MASCARA results. For the 50lpm flow rate, DRACCAR calculated the same velocity profile observed in the experiments, but it underestimated the axial velocity in the balloon and the second transition zone, finding the minimum earlier. Finally, DRACCAR overestimated the axial velocity for the sub-channel C with the G90%/240mm bundle as we observed

with G61%/100mm.

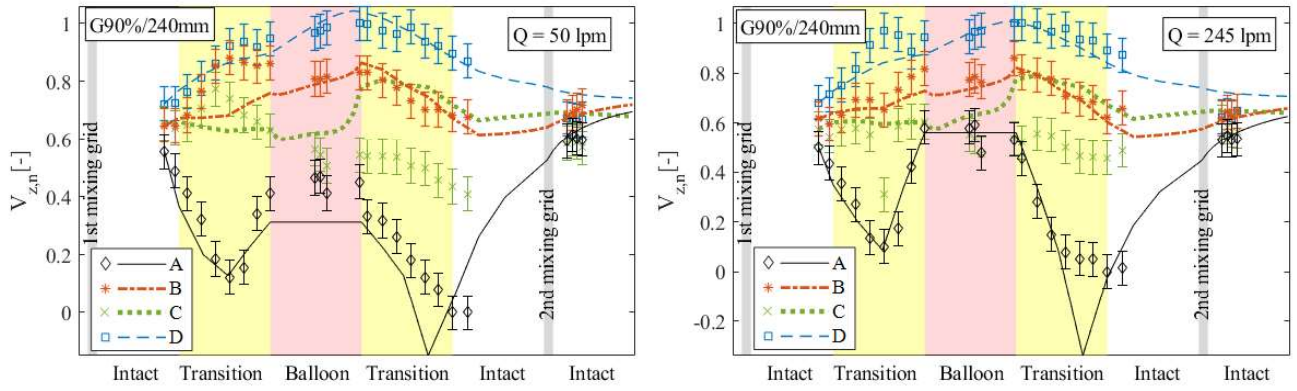

(a) (b)

Figure 13: Normalized velocities (lines are DRACCAR simulations, markers are MASCARA results) in different sub-channels for the G90%/240mm bundle: (a) 50 lpm, and (b) 245 lpm.

Although MASCARA experiments may appear relatively simple for a computational fluid dynamics simulation, we should remind that DRACCAR calculations rely on models describing the fluid behavior inside the entire sub-channel at a given axial position, so the velocity field inside this sub-channel is not calculated. This lack of resolution within the sub-channel makes the calculation of the Navier-Stokes equation becomes more complicated, especially because of the convective term ($V.\nabla V$) in the Lagrangian derivative. This term is significant in-between and within the sub-channels in the transition zones, where, in fact, DRACCAR was less accurate (see Figs. 12 and 13). Although the axial velocity estimates for sub-channel C all along with the bundle and sub-channel A in the second transition zone were less accurate, with deviations higher than the experimental uncertainty, DRACCAR succeeded to calculate precisely most of the velocity points. Table 2 presents the percentage of axial velocity points that DRACCAR could estimate within a range of ±15% of MASCARA's axial velocities values for each bundle, flow rate and sub-channel. For this table, the real MASCARA and DRACCAR velocities were used (not normalized velocities). As we discussed, the calculations for the sub-channel A, the one in the center of the balloon, were in general quite accurate (except for G90%/240mm with 50 lpm). For less blocked sub-channels, namely B and D, DRACCAR estimated more than 80% of the local axial velocities within a range of ±15% with respect to the MASCARA value. As already mentioned, the calculations for sub-channel C (partially blocked by the neighboring balloon and a guide tube) were not accurate enough, which deserves more attention to improve the model in this case, even though this sub-channel is not considered critical as the axial velocity is not much reduced because of the flow redistribution. A more precise analysis of the transverse velocities may help to explain this difference between calculation and experimental data.

With the present results, it was found that the fluid dynamics model implemented in DRACCAR was capable of predicting most of the axial velocity of the sub-channels in both blocked assemblies. However, there are still aspects of DRACCAR to improve, especially in the calculation of the sub-channels' axial velocity near the guide tubes (as sub-channel C).

Table 2: Percentage of points estimated by DRACCAR between a range of ±15% of the MASCARA results.

	G61%/100mm		G90%/240mm	
Flow (lpm)	50	245	50	245
Sub-channel A	83%	69%	20%	68%
Sub-channel B	100%	100%	80%	100%
Sub-channel C	58%	72%	40%	56%
Sub-channel D	100%	100%	100%	100%
Total	85%	85%	60%	81%

6. Conclusions

In this study, we compared the IRSN DRACCAR LOCA code simulations with test results from the MASCARA experimental campaign for two ballooned 7 x 7 bundles with different blockage ratios and lengths (bundles G61%/100mm G90%/240mm) and with different flow rates, one in laminar regime (50 lpm) and the other in turbulent regime (245 lpm). The results showed that DRACCAR succeeded to estimate the axial flow velocity in intact and less blocked sub-channels for both configurations and flow rates. For the blocked sub-channel in the center of the balloon, DRACCAR performed better for the less blocked bundle (G61%/100mm). In this case, DRACCAR succeeds to correctly estimate the velocity profile for this blocked sub-channel and most of the points were estimated within the experimental uncertainty; however, the axial velocity was largely overestimated at the end of the second transition zone. For the more blocked bundle (G90%/240mm), which is considered one of the worst-case scenarios of clad ballooning during a LOCA, DRACCAR correctly estimates the velocity behavior in this sub-channel, however it underestimate MASCARA's velocity from the blocked zone. Nonetheless, this would results in a conservative heat transfer estimation. Finally, for the partially-blocked sub-channel neighboring the balloon and a guide tube, the axial velocity estimate deserves more attention to improve its calculation, even though this is not considered a critical sub-channel during a LOCA.

Once COAL experimental campaign will be finished, simulations of the experiments will be performed with DRACCAR including all the involved thermal-hydraulics phenomena during the reflooding phase, which will be an important step for the validation of code. Furthermore, DRACCAR simulations of MASCARA experiments with non-coplanar balloons are also expected, in which balloons are located in different axial positions so the flow redistribution behaves differently from those presented in this study.

7. Acknowledgement

The authors would like to thank Didier Stemmelen, Research Fellow at CNRS and LEMTA (Université de Lorraine), for reviewing this paper and giving valuable suggestions to improve its quality, especially concerning the method and result presentations.

8. Funding

This work is completed within the framework of RSNR Project PERFROI from a French State aid managed by the French National Research Agency under the program of Investments for the Future carrying the reference n° ANR-11-RSNR-0017.

References

[1] G. Repetto, C. Dominguez, B. Durville, S. Carnemolla, D. Campello, C. Tardif, M. Gradeck, The R&D PERFROI project on thermal mechanical and thermal hydraulics behaviors of a fuel rod assembly during a loss of coolant accident, 16th International Topical Meeting on Nuclear Reactor Thermal Hydraulics (NURETH-16) 1 (2015) 1–14.

[2] Y. Jin, F. R. Beck, B. R. Lowery, D. J. Miller, F. B. Cheung, S. M. Bajorek, K. Tien, C. L. Hoxie, Experimental study of droplet sizes across a spacer grid location under various reflood conditions, Experimental Thermal and Fluid Science 94 (February 2017) (2018) 246–257. doi:10.1016/j.expthermflusci.2018.02.017.

[3] H. K. Cho, K. Y. Choi, S. Cho, C.-H. Song, Experimental observation of the droplet size change across a wet grid spacer in a 6×6 rod bundle, Nuclear Engineering and Design 241 (12) (2011) 4649–4656. doi:https://doi.org/10.1016/j.nucengdes.2011.03.042.

[4] Y. Jin, F.-B. Cheung, K. Shirvan, S. M. Bajorek, K. Tien, C. L. Hoxie, Development of a droplet breakup model for dry spacer grid in the dispersed flow film boiling regime during reflood transients, International Journal of Heat and Mass Transfer 143 (2019) 118544. doi:https://doi.org/10.1016/j.ijheatmasstransfer.2019.118544.

[5] J. M. Yoo, B. J. Yun, H. Y. Yoon, J. J. Jeong, Modeling of the droplet entrainment rate in the post-dryout regime for the analysis of a reflood phase, Annals of Nuclear Energy 148 (2020) 107757. doi:https://doi.org/10.1016/j.anucene.2020.107757.

[6] J. Peña Carrillo, A. V. S. Oliveira, A. Labergue, T. Glantz, M. Gradeck, Experimental thermal hydraulics study of the blockage ratio effect during the cooling of a vertical tube with an internal steam-droplets flow, International Journal of Heat and Mass Transfer 140 (2019) 648 – 659. doi:https://doi.org/10.1016/j.ijheatmasstransfer.2019.06.012.

[7] A. V. S. Oliveira, J. D. Peña Carrillo, A. Labergue, T. Glantz, M. Gradeck, Experimental study of dispersed flow film boiling at sub-channel scale in LOCA conditions: Influence of the steam flow rate and residual power, Applied Thermal Engineering 172 (2020) 115143. doi:https://doi.org/10.1016/j.applthermaleng.2020.115143.

[8] N. H. Nguyen, J. Kim, S.-H. Hong, S.-K. Moon, C.-H. Song, Improvements of cobra-tf on the effect of flow blockage during a lb loca with consideration of fuel relocation phenomenon, Nuclear Engineering and Design 325 (2017) 218 – 231. doi:https://doi.org/10.1016/j.nucengdes.2017.08.015.

[9] P. Ruyer, N. Seiler, B. Biton, F. Lelong, F. Secondi, D. Baalbaki, M. Gradeck, Two-phase flow across a partially damaged core during the reflood phase of a LOCA, Nuclear Engineering and Design 264 (2013) 187 – 194, SI:NURETH-14. doi:https://doi.org/10.1016/j.nucengdes.2013.02.026.

[10] A. V. S. Oliveira, J. D. Peña Carrillo, A. Labergue, T. Glantz, M. Gradeck, Mechanistic modeling of the thermal-hydraulics in polydispersed flow film boiling in LOCA conditions, Nuclear Engineering and Design 357 (2020) 110388. doi:https://doi.org/10.1016/j.nucengdes.2019.110388.

[11] Y. Guo, K. Mishima, A non-equilibrium mechanistic heat transfer model for post-dryout dispersed flow regime, Experimental Thermal and Fluid Science 26 (6-7) (2002) 861–869. doi:10.1016/S0894-1777(02)00195-4.

[12] C.-H. Song, Some issues and challenges in advanced thermal-hydraulic safety research, Nuclear Technology 196 (3) (2016) 421–445. doi:https://doi.org/10.13182/NT16-91.

[13] G. Repetto, T. Glantz, G. Guillard, B. Bruyère, Q. Grando, Core coolability in loss of coolant accident: the COAL experiments investigating the thermal hydraulics of a rod bundle with blocked area during the reflooding, 17th International Topical Meeting on Nuclear Reactor Thermal Hydraulics (NURETH-17) 1 (2017) 359–372.

[14] G. Repetto, C. Marquié, B. Bruyère, T. Glantz, Core coolability in loss of coolant accident: the COAL experiments, 16th International Topical Meeting on Nuclear Reactor Thermal Hydraulics (NURETH-16) 1 (2015) 24–37.

[15] S. Bascou, O. De Luze, S. Ederli, G. Guillard, Development and validation of the multi-physics DRACCAR code, Annals of Nuclear Energy 84 (2015) 1–18. doi:10.1016/j.anucene.2014.09.040.

[16] T. Glantz, T. Taurines, O. De Luze, S. Belon, G. Guillard, F. Jacq, DRACCAR: A multi-physics code for computational analysis of multi-rod ballooning, coolability and fuel relocation during LOCA transients Part one: General modeling description, Nuclear Engineering and Design 339 (June) (2018) 269–285. doi:10.1016/j.nucengdes.2018.06.022.

[17] T. Glantz, T. Taurines, S. Belon, O. De Luze, G. Guillard, F. Jacq, DRACCAR: A multi-physics code for computational analysis of multi-rod ballooning, coolability and fuel relocation during LOCA transients. Part Two: Overview of modeling capabilities for LOCA, Nuclear Engineering and Design 339 (August) (2018) 202–214. doi:10.1016/j.nucengdes.2018.08.031.

[18] A. V. S. Oliveira, D. Stemmelen, S. Leclerc, T. Glantz, A. Labergue, G. Repetto, M. Gradeck, Parametric effects on the flow redistribution in ballooned bundles evaluated by magnetic resonance velocimetry, Experimental Thermal and Fluid Science 125 (2021) 110383. doi:https://doi.org/10.1016/j.expthermflusci.2021.110383.

[19] A. V. S. Oliveira, D. Stemmelen, S. Leclerc, T. Glantz, A. Labergue, G. Repetto, M. Gradeck, Velocity field and flow redistribution in a ballooned 7×7 fuel bundle measured by magnetic resonance velocimetry, Nuclear Engineering and Design 369 (2020) 110828. doi:https://doi.org/10.1016/j.nucengdes.2020.110828.

[20] P. Chatelard, S. Belon, L. Bosland, L. Carénini, O. Coindreau, F. Cousin, C. Marchetto, H. Nowack, L. Piar, L. Chailan, Main modelling features of the astec v2.1 major version, Annals of Nuclear Energy 93 (2016) 83–93, eRMSAR-2015 conference of SARNET in the frame of the NUGENIA Technical Area 2. doi:https://doi.org/10.1016/j.anucene.2015.12.026.

[21] P. Emonot, A. Souyri, J. Gandrille, F. Barré, Cathare-3: A new system code for thermal-hydraulics in the context of the neptune project, Nuclear Engineering and Design 241 (11) (2011) 4476–4481, 13th International Topical Meeting on Nuclear Reactor Thermal Hydraulics (NURETH-13). doi:https://doi.org/10.1016/j.nucengdes.2011.04.049.

[22] J. D. Peña Carrillo, A. V. S. Oliveira, T. Glantz, G. Repetto, M. Gradeck, Analyse des transferts thermiques d'un écoulement vertical vapeur/gouttes dans une géométrie tubulaire, in: Congrès français de thermique, Société Française de Thermique, Nantes, 2019.

[23] C. Grandjean, Coolability of blocked regions in a rod bundle after ballooning under LOCA conditions: Main findings from a review of past experimental programmes, Nuclear Engineering and Design 237 (15) (2007) 1872–1886. doi:https://doi.org/10.1016/j.nucengdes.2007.02.022.
URL https://www.sciencedirect.com/science/article/pii/S0029549307002038

[24] R. Prea, V. Figerou, A. Mekkas, A. Ruby, Cathare-3: A first computation of a 3-inch-break loss-of-coolant accident using both Cartesian and cylindrical 3D-meshes modeling of a PWR vessel, in: 17th International Topical Meeting on Nuclear Reactor Thermal Hydraulics, NURETH 2017, Vol. 2017-Septe, 2017.

[25] I. Idel'cik, Mémento des pertes de charges, 3rd Edition, Eyrolles, EDF, Paris, 1986.

Declaration of Interest Statement

Declaration of interests

☒ The authors declare that they have no known competing financial interests or personal relationships that could have appeared to influence the work reported in this paper.

☐The authors declare the following financial interests/personal relationships which may be considered as potential competing interests:

Credit Author Statement

J.E. Luna Valencia: Data Curation, Investigation, Writing - Original draft preparation

Arthur V. S. Oliveira: Methodology, Data Curation, Investigation, Writing - Original draft preparation

T. Glantz: Data Curation, Conceptualization, Software, Supervision, Writing - Review & Editing

A. Labergue: Supervision, Writing - Review & Editing

S. Leclerc: Methodology, Software, Investigation, Writing - Review & Editing

M. Gradeck: Conceptualization, Supervision, Project administration, Writing - Review & Editing

References

[1] G. Repetto, C. Dominguez, B. Durville, S. Carnemolla, D. Campello, C. Tardif, M. Gradeck, The R&D PER- FROI project on thermal mechanical and thermal hydraulics behaviors of a fuel rod assembly during a loss ofcoolant accident, 16th International Topical Meeting on Nuclear Reactor Thermal Hydraulics (NURETH-16) 1 (2015) 1–14.

[2] Y. Jin, F. R. Beck, B. R. Lowery, D. J. Miller, F. B. Cheung, S. M. Bajorek, K. Tien, C. L. Hoxie, Experimentalstudy of droplet sizes across a spacer grid location under various reflood conditions, Experimental Thermal and Fluid Science 94 (February 2017) (2018) 246–257. doi:10.1016/j.expthermflusci.2018.02.017.

[3] H. K. Cho, K. Y. Choi, S. Cho, C.-H. Song, Experimental observation of the droplet size change across a wet gridspacer in a 6x6 rod bundle, Nuclear Engineering and Design 241 (12) (2011) 4649 – 4656, the 18th International Conference on Nuclear Engineering (ICONE-18). doi:https://doi.org/10.1016/j.nucengdes.2011.03.042.

[4] Y. Jin, F.-B. Cheung, K. Shirvan, S. M. Bajorek, K. Tien, C. L. Hoxie, Development of a droplet breakup model for dry spacer grid in the dispersed flow film boiling regime during reflood transients, International Journal of Heat and Mass Transfer 143 (2019) 118544. doi:https://doi.org/10.1016/j.ijheatmasstransfer.2019.118544.

[5] J. M. Yoo, B. J. Yun, H. Y. Yoon, J. J. Jeong, Modeling of the droplet entrainment rate in the post-dryout regime for the analysis of a reflood phase, Annals of Nuclear Energy 148 (2020) 107757. doi:https://doi. org/10.1016/j.anucene.2020.107757.

[6] J. Peña Carrillo, A. V. S. Oliveira, A. Labergue, T. Glantz, M. Gradeck, Experimental thermal hydraulics study of the blockage ratio effect during the cooling of a vertical tube with an internal steam-droplets flow, International Journal of Heat and Mass Transfer 140 (2019) 648 – 659. doi:https://doi.org/10.1016/j. ijheatmasstransfer.2019.06.012.

[7] A. V. S. Oliveira, J. D. Peña Carrillo, A. Labergue, T. Glantz, M. Gradeck, Experimental study of dispersed flow film boiling at sub-channel scale in LOCA conditions: Influence of the steam flow rate and residual power, Applied Thermal Engineering 172 (2020) 115143. doi:https://doi.org/10.1016/j.applthermaleng.2020. 115143.

[8] N. H. Nguyen, J. Kim, S.-H. Hong, S.-K. Moon, C.-H. Song, Improvements of cobra-tf on the effect of flow blockage during a lb loca with consideration of fuel relocation phenomenon, Nuclear Engineering and Design 325 (2017) 218 – 231. doi:https://doi.org/10.1016/j.nucengdes.2017.08.015.

[9] P. Ruyer, N. Seiler, B. Biton, F. Lelong, F. Secondi, D. Baalbaki, M. Gradeck, Two-phase flow across a partially damaged core during the reflood phase of a LOCA, Nuclear Engineering and Design

264 (2013) 187 – 194, SI:NURETH-14. doi:https://doi.org/10.1016/j.nucengdes.2013.02.026.

[10] A. V. S. Oliveira, J. D. Peña Carrillo, A. Labergue, T. Glantz, M. Gradeck, Mechanistic modeling of the thermal- hydraulics in polydispersed flow film boiling in LOCA conditions, Nuclear Engineering and Design 357 (2020) 110388. doi:https://doi.org/10.1016/j.nucengdes.2019.110388.

[11] Y. Guo, K. Mishima, A non-equilibrium mechanistic heat transfer model for post-dryout dispersed flow regime, Experimental Thermal and Fluid Science 26 (6-7) (2002) 861–869. doi:10.1016/S0894-1777(02)00195-4.

[12] C.-H. Song, Some issues and challenges in advanced thermal-hydraulic safety research, Nuclear Technology196 (3) (2016) 421–445. doi:https://doi.org/10.13182/NT16-91.

[13] G. Repetto, T. Glantz, G. Guillard, B. Bruy`ere, Q. Grando, Core coolability in loss of coolant accident: the COAL experiments investigating the thermal hydraulics of a rod bundle with blocked area during the reflooding,17th International Topical Meeting on Nuclear Reactor Thermal Hydraulics (NURETH-17) 1 (2017) 359–372.

[14] G. Repetto, C. Marquié, B. Bruyère, T. Glantz, Core coolability in loss of coolant accident: the COAL exper- iments, 16th International Topical Meeting on Nuclear Reactor Thermal Hydraulics (NURETH-16) 1 (2015) 24–37.

[15] S. Bascou, O. De Luze, S. Ederli, G. Guillard, Development and validation of the multi-physics DRACCAR code, Annals of Nuclear Energy 84 (2015) 1–18. doi:10.1016/j.anucene.2014.09.040.

[16] T. Glantz, T. Taurines, O. De Luze, S. Belon, G. Guillard, F. Jacq, DRACCAR: A multi-physics code for computational analysis of multi-rod ballooning, coolability and fuel relocation during LOCA transients Part one: General modeling description, Nuclear Engineering and Design 339 (June) (2018) 269–285. doi:10.1016/j.nucengdes.2018.06.022.

[17] T. Glantz, T. Taurines, S. Belon, O. De Luze, G. Guillard, F. Jacq, DRACCAR: A multi-physics code for computational analysis of multi-rod ballooning, coolability and fuel relocation during LOCA transients. Part Two: Overview of modeling capabilities for LOCA, Nuclear Engineering and Design 339 (August) (2018) 202– 214. doi:10.1016/j.nucengdes.2018.08.031.

[18] A. V. S. Oliveira, D. Stemmelen, S. Leclerc, T. Glantz, A. Labergue, G. Repetto, M. Gradeck, Parametric effects on the flow redistribution in ballooned bundles evaluated by magnetic resonance velocimetry, Experimental Thermal and Fluid Science 125 (2021) 110383. doi:https://doi.org/10.1016/j.expthermflusci.2021. 110383.

[19] A. V. S. Oliveira, D. Stemmelen, S. Leclerc, T. Glantz, A. Labergue, G. Repetto, M. Gradeck, Velocity field and flow redistribution in a ballooned 7×7 fuel bundle measured by magnetic resonance velocimetry, Nuclear Engineering and Design 369 (2020) 110828.

doi:https://doi.org/10.1016/j.nucengdes.2020.110828.

[20] P. Chatelard, S. Belon, L. Bosland, L. Carénini, O. Coindreau, F. Cousin, C. Marchetto, H. Nowack, L. Piar, L. Chailan, Main modelling features of the astec v2.1 major version, Annals of Nuclear Energy 93 (2016)83–93, eRMSAR-2015 conference of SARNET in the frame of the NUGENIA Technical Area 2. doi:https://doi.org/10.1016/j.anucene.2015.12.026.

[21] P. Emonot, A. Souyri, J. Gandrille, F. Barré, Cathare-3: A new system code for thermal-hydraulics in the context of the neptune project, Nuclear Engineering and Design 241 (11) (2011) 4476–4481, 13th International Topical Meeting on Nuclear Reactor Thermal Hydraulics (NURETH-13). doi:https://doi.org/10.1016/j. nucengdes.2011.04.049.

[22] J. D. Peña Carrillo, A. V. S. Oliveira, T. Glantz, G. Repetto, M. Gradeck, Analyse des transferts thermiques d'un écoulement vertical vapeur/gouttes dans une géométrie tubulaire, in: Congrès français de thermique, Société Française de Thermique, Nantes, 2019.

[23] C. Grandjean, Coolability of blocked regions in a rod bundle after ballooning under LOCA conditions: Main findings from a review of past experimental programmes, Nuclear Engineering and Design 237 (15) (2007) 1872 – 1886, NURETH-11. doi:https://doi.org/10.1016/j.nucengdes.2007.02.022.

[24] R. Prea, V. Figerou, A. Mekkas, A. Ruby, Cathare-3: A first computation of a 3-inch-break loss-of-coolantaccident using both Cartesian and cylindrical 3D-meshes modeling of a PWR vessel, in: 17th InternationalTopical Meeting on Nuclear Reactor Thermal Hydraulics, NURETH 2017, Vol. 2017-Septe, 2017.

[25] Idel'cik, Mémento des pertes de charges, 3rd Edition, Eyrolles, EDF, Paris, 1986.